

We thank anonymous referee #1 for his or her comments, and for taking the time to review our manuscript. We've noticed discrepancies in line numbers and figure references, however we believe that we've identified all of places the referee is referring to. We've copied the referee's comments in blue. Our responses are in red.

update 11/13/2019 – we've added line numbers and references to the revision

In this study, snow in the upper Amu Darya and Indus basins is modeled using multiple techniques and a newly available snow depth data record. These data and results provide insight into the likely range of snow depths and snowpack properties in a region where there was previously very limited understanding. The study is well researched and designed and the paper is well written. I think this is a good contribution to the snow research literature for HMA, and provides evaluation of some potential tools that could be used for avalanche prediction. I have some minor suggestions and comments for consideration.

Line 87: Instead of “snow on land melt” use “terrestrial snow melt”

We assume this is referring to l 87. The term used in cited Armstrong et al (2019) reference is “snow on land”, so we'd like to keep this as is for consistency.

Line 143: Move the reference for APHRODITE to the earlier section (lines 110-111) where all the other global precipitation products are referenced.

Again, the line reference appears transposed. We assume this is referring to l 134. And yes, we will move the Yatagai et al reference up.

106 ...APHRODITE [*Yatagai et al., 2012*]

Table 1: It is not clear to me why Alpine3D and NOAH MP are run at 25km resolution. Why not run at a higher resolution for direct comparison?

This was driven by the GLDAS and NOAHMP model resolution. GLDAS is available at 0.25° or 27.7 km in the north-south direction. For NOAH MP, the forcings used were from MERRA-2 at 0.625° x 0.5°. 25 km the highest resolution we felt comfortable comparing.

Section 4.4 It's not clear how the AKAH stations are combined with SNOWPACK. Are the observations directly inserted and the model is used to estimate other snow properties (i.e. density, grain size, etc)? Ok, I see in the appendix that it is used as precipitation. I think that should be mentioned in the paper.

We assume you are referring to Section 5.4. In Table 1, under the SNOWPACK row, it says that the AKAH snow measurements were used as forcings along with downscaled forcings from ParBal. This is shown graphically in Figure 2. We will however, reiterate this in the text since it was not clear.

184-198 Previous results with SNOWPACK [*Bair et al., 2018*] show high model sensitivity to precipitation, but only a 1% error in modeled SWE when using snow depth only (not total precipitation) as a forcing. Thus, given reliable snow depth measurements at each AKAH station (see Section 5.4), modeled SWE during the accumulation season is treated as having negligible

uncertainty. During the ablation season (after peak SWE), uncertainty is higher. Unlike during snow accumulation events, SNOWPACK does not force its modeled snow ablation to match the measured snow depth decreases. Uncertainty in SWE during the ablation season is then largely dependent on radiative forcings [Marks and Dozier, 1992] and the broadband snow albedo [Bair *et al.*, 2019]. Here, 5% uncertainty is used, based on the MAE from SWE reconstructions using the same remotely-sensed forcings at a continental sub-alpine site [Bair *et al.*, 2019]. In the same study, a small (3%) bias in SWE was also found, but this is likely due to shortcomings with the reconstruction method and not applicable to SWE modeled with SNOWPACK. Thus, the small bias was ignored. We acknowledge that these uncertainty estimates are themselves uncertain, e.g. the reanalysis forcings could be especially poor for this region compared to those available in the western US.

Line 266: should this date be “2018-4-1”?

On l 264 and elsewhere throughout the manuscript we were asked to use the international date format by the Editor, which is “1 April 2017” for that date.

Line 316: remove “are” after values, so it reads “median values between years are a week apart”

Ah, thanks for spotting. We will remove the typo.

348-349 ... but the median values between years are a week apart

Figure 3: I would be interested in seeing a spatial comparison of the individual stations, particularly in 2017. Are there certain stations where most of the disagreement occurs, or it is similarly biased at all stations?

We are not clear about potential biases in this figure. Perhaps you are referring to Figures 4 & 5, not Figure 3? In any case, we didn't find any spatial trends. Figure 5 summarizes the error distribution and shows that most stations are slightly negatively biased (blue box is 25<sup>th</sup>-75<sup>th</sup> percentile).

Line 355-356: you say, “The ParBal results are confounding given that the agreement between the modeled SWE from ParBal and SNOWPACK at individual AKAH stations is much better for both 2017 and 2018.” The agreement for 2018 shown in Figure 3 is good, but in 2017 there is quite a large bias – similar to what is seen in Figure 5 for the whole study area.

The differences between the four models in 2017 at 25 km shown in Figure 6 were much greater than the differences between ParBal and SNOWPACK at the point scale, shown in Figure 4. In 2017, for the four models, NOAH MP showed 234% of ParBal, Alpine 3D showed 195% of ParBal, and GLDAS-2 showed 146% of ParBal. In contrast, SNOWPACK showed 128% of ParBal at the point scale in 2017. Thus, we still find that the agreement between ParBal and SNOWPACK at the point scale was much better than between ParBal and the other 3 models at 25 km.

Figure 6: The Alpine 3D images shows considerably less SCA than the ParBal estimate. Since the Alpine 3D estimate is using the gage data I assume where it shows no snow, the snow depth reported at those sites was zero. Is that correct? The ParBal estimate is using MODIS

data, which is presumably showing snow in those areas on that date. I'm surprised there is such a large difference. In fact, looking at the movie there is consistently a large difference in snow extent between those two estimates, even at the lower elevations where there are more stations. Why do you think that is?

We assume this is in reference to Figure 7. Because of the austerity of this region, none of these models use gauge data because it's generally not available, hence all of the reanalysis-based forcings. We agree that ParBal (the only model driven by remotely-sensed snow measurements) shows more SCA that persists longer into the melt season than Alpine3D. There are many factors that could cause this, but we suggest the most likely is inaccurate precipitation extrapolation, as we discuss on l 351-352. Thus, too much precipitation is placed in some cells, and too little in others. This extrapolation problem stems from the fact that all of these stations are located in valley floors, which are lower than the average grid cell elevations (l 333-335).

393-398 For example, the Alpine3D pixels seem to melt out early compared to the other models, especially ParBal, which is the only model relying on satellite-based estimates of fSCA (see supplementary video). Thus, Alpine3D may be placing too little SWE in cold, high elevation areas that melt slowly. These problems are all indicative of stations that are located in valley bottoms and that only cover the lowest elevations across these 25 km pixels.

Line 404: Is there a reference you can add for the statement "Compared to a previous effort. . ."? Not sure what this is referring to.

Section 4 "PREVIOUS WORK WITH AKAH SNOW MEASUREMENTS" contains two paragraphs about this.

- Bair, E. H., R. E. Davis, and J. Dozier (2018), Hourly mass and snow energy balance measurements from Mammoth Mountain, CA USA, 2011–2017, *Earth Syst. Sci. Data*, 10(1), 549-563, doi: 10.5194/essd-10-549-2018.
- Bair, E. H., K. Rittger, S. M. Skiles, and J. Dozier (2019), An Examination of Snow Albedo Estimates From MODIS and Their Impact on Snow Water Equivalent Reconstruction, *Water Resources Research*, 55(9), 7826-7842, doi: 10.1029/2019wr024810.
- Marks, D., and J. Dozier (1992), Climate and energy exchange at the snow surface in the alpine region of the Sierra Nevada, 2, Snow cover energy balance, *Water Resources Research*, 28(11), 3043-3054, doi: 10.1029/92WR01483.
- Yatagai, A., K. Kamiguchi, O. Arakawa, A. Hamada, N. Yasutomi, and A. Kitoh (2012), APHRODITE: Constructing a Long-Term Daily Gridded Precipitation Dataset for Asia Based on a Dense Network of Rain Gauges, *Bulletin of the American Meteorological Society*, 93(9), 1401-1415, doi: 10.1175/bams-d-11-00122.1.

We thank anonymous referee #2 for his or her comments, and for taking the time to review our manuscript. We've copied the referee's comments in blue. Our responses are in red.

update 11/13/2019 – we've added line numbers and references to the revision

The authors present a study using three different models computing SWE for the Hindukush-Pamir region, as well as snow stratigraphy for selected locations and are able to compare point scale simulations to large scale datasets. The topic is of great importance (as they point out, the region has seen very little attention in the direction of snow even though it is understood to be a major driver of streamflow and important to understand droughts/floods in both Pakistan and Afghanistan) and generally very little field data is available or accessible. The main advancement of the study is the availability of a large number of snow depth measurements from the region.

I find the study (a) in general of great value for the community and The Cryosphere in its proposed scope, (b) covering an area that desperately needs more data analysis and (c) generally clearly written and of solid scientific quality. However I would like to see my major concerns I detail below addressed before I find it acceptable for publication.

Major concern:

I appreciate that getting field data as shown here is very hard to collect and once stored by on site staff, often difficult to impossible to obtain. That the authors managed to do so is impressive and I know the general hesitation of local institutions to provide any such sets. However I fear that this does not absolve authors of scientific studies to (a) ascertain the data quality and (b) if not provide then visualize the data to the reader. The authors themselves are cautious with the data quality (L216: 'appeared to be most reliable . . .'). This warrants an assessment of the quality, how that is assessed, what the 'good' data looks like (incl uncertainty) and eventually how this data quality affects model outcomes in ParBal/SNOWPACK. AKAH has excellent staff and can be considered among the most reliable institutes in this area, but many of the stations shown (like the one in the Little Wakhan or north of Ishkashem on the Afghan side) are in areas hardly accessible at all and I wonder how this data was recorded at daily intervals and quality checked internally. I have checked the earlier paper and the report on the avalanche program and equally fail to find details there.

We agree that the AKAH measurement quality concerns are valid. We extensively discuss the quality of the manual daily AKAH snow depth measurements in Section 5.4 where we cover all of the quality issues. Thus, we have already addressed point a). Regarding point b), we find that plotting the errors in the AKAH snow depth is unnecessary, as they are extensively described. For example, one of the most common errors was spurious drops with zeros instead of null values (l 230-232). We do not agree that these need to be plotted for the reader to understand what we are referring to. In terms of internal quality checks from AKAH, as far as we are aware, there were none. We will state this in a revision of the manuscript.

248-249 To our knowledge, no quality control was performed on the AKAH station measurements before we received them.

Further, in a revision, we will expand on what is stated on l 217; that is when total snow depth measurements were recorded and did not show spurious drops (there were no spikes – consistent with manual vs. automated acoustic snow depth measurements), that the data quality



is likely high and the snow depth is accurate at that point. The only likely error from manually reading a total depth stake measurement is a transcription error, which would show up as a drop or spike.

184-188 Previous results with SNOWPACK [Bair *et al.*, 2018a] show high model sensitivity to precipitation, but only a 1% error in modeled SWE when using snow depth only (not total precipitation) as a forcing. Thus, given reliable snow depth measurements at each AKAH station (see Section 5.4), modeled SWE during the accumulation season is treated as having negligible uncertainty.

252-253 Apart from spurious drops or missing values (see below), the HS measurement appeared consistent and believable at most of the stations, implying an accurate snow depth record.

We will emphasize in a revised manuscript that the errors in ParBal are completely independent of the manually measured AKAH snow depth, as ParBal does not use in situ measurements. The errors in ParBal are mostly based on the fractional snow covered area and radiative forcings, and are covered extensively in the cited prior publications [Bair *et al.*, 2016; Rittger *et al.*, 2016]. By “earlier paper”, perhaps the reviewer is citing Bair *et al.* [2018b], which focuses on the machine learning approach, but not on the sources of errors in the ParBal model ?

218-224 The errors in SWE from ParBal are mostly from fSCA and the radiative forcings. Errors and details on ParBal are covered extensively in Bair *et al.* [2016] and Rittger *et al.* [2016]. In the supplement for Bair *et al.* [2018b], the errors arising from using GLDAS-2 and CERES 4a (available worldwide but at coarser spatial resolution) vs. NLDAS-2 are specifically evaluated. Using three years of basin-wide SWE estimated by the Airborne Snow Observatory in the upper Tuolumne Basin, California USA, the MAE for ParBal was 25 mm or 26% [Bair *et al.*, 2018b].

We will add uncertainty bounds on the red and blue SWE curves shown in Figure 4 in a revised manuscript. The range of SWE in the 9-pixel neighborhood around each AKAH station (I 295-297) will be used to create the bounds around the red ParBal curve. For the blue SNOWPACK curve, because we find the AKAH snow depth to be accurate (see above), we also find the accumulation season SWE modeled by SNOWPACK at that point to be accurate. We justify this assumption using results from Bair *et al.* [2018a], where it is shown that the peak SWE modeled by SNOWPACK at a site with little melt during the accumulation season (which seems to be the case for the AKAH stations based on measured depth) is mostly dependent on the precipitation forcing. A similar result is shown in Bartelt and Lehning [2002].

For the ablation season, there is considerable uncertainty in the blue SNOWPACK curve caused by the radiative forcings and the snow albedo parameterization. Given a lack of knowledge of the uncertainties in the radiative forcings for this region, we will use the 4-6% RMSE and negligible bias reported for our remotely-sensed albedos reported in a recent study [Bair *et al.*, 2019]. These errors led to a 5% mean absolute error and 3% bias in ablation season SWE for a continental site in CO USA [Bair *et al.*, 2019].

184-198 Previous results with SNOWPACK [Bair *et al.*, 2018a] show high model sensitivity to precipitation, but only a 1% error in modeled SWE when using snow depth only (not total precipitation) as a forcing. Thus, given reliable snow depth measurements at each AKAH station (see Section 5.4), modeled SWE during the accumulation season is treated as having negligible

uncertainty. During the ablation season (after peak SWE), uncertainty is higher. Unlike during snow accumulation events, SNOWPACK does not force its modeled snow ablation to match the measured snow depth decreases. Uncertainty in SWE during the ablation season is then largely dependent on radiative forcings [Marks and Dozier, 1992] and the broadband snow albedo [Bair et al., 2019]. Here, 5% uncertainty is used, based on the MAE from SWE reconstructions using the same remotely-sensed forcings at a continental sub-alpine site [Bair et al., 2019]. In the same study, a small (3%) bias in SWE was also found, but this is likely due to shortcomings with the reconstruction method and not applicable to SWE modeled with SNOWPACK. Thus, the small bias was ignored. We acknowledge that these uncertainty estimates are themselves uncertain, e.g. the reanalysis forcings could be especially poor for this region compared to those available in the western US.

332-333 We also include the high and low SWE values in that surrounding 9-pixel neighborhood to bound the uncertainty.

356-357 The high/low values in the 9-pixel neighborhood show the wide spatial variation in SWE estimates, and are to be expected in these deep valley sites (Section 6.2).

Revised Figure 4

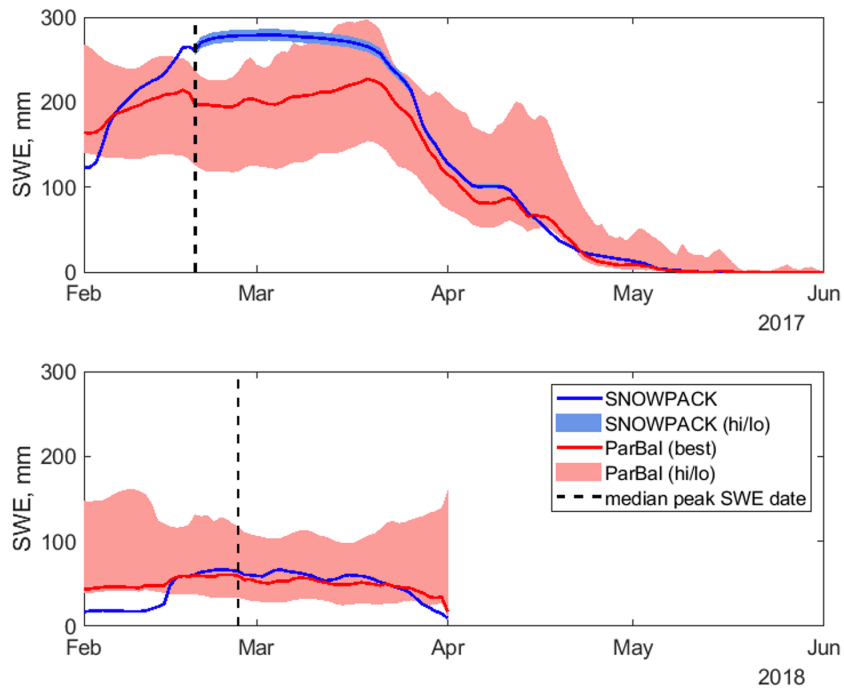


Figure 4 Mean SWE for 2017 (a) and 2018 (b) modeled at all of the AKAH stations using SNOWPACK (blue lines) compared to reconstructed SWE from ParBal using a best of 9-pixel approach (red lines). Also plotted is the median peak SWE date. The hi/lo bounds (filled areas) represent uncertainty. For ParBal, uncertainty is expressed as the range of values in the 9 pixel neighborhood. For SNOWPACK, uncertainty is 5% of the modeled SWE during the ablation season. See 5.1 and 5.2 for details. The modeled SWE values end abruptly on 1 April 2018 because the AKAH stations stopped reporting due to drought conditions. The number of stations used is the same as Figure 3.

I also find it problematic to sell the story as a ‘validation of models with measurements’, as the snow depth measurements are used as an input for one model (ParBal, equally dependent on other remote sensing data but which I think is being understood as the ‘validation data’ here) that is then compared to another (SNOWPACK/ALPINE3D).

As shown in [Bair *et al.*, 2018a] and Bartelt and Lehning [2002], given accurate snow depth measurements, which we believe to be the case for the cleaned AKAH stations, the accumulation season SWE can be well modeled. For the SNOWPACK and ParBal comparisons, we consider the SNOWPACK modeled SWE as legitimate validation data because it is the snow depth, not its density, that drives the variability in SWE. This has been pointed out repeatedly in The Airborne Snow Observatory (ASO) project [Painter *et al.*, 2016] who show that the CV for depth is ~ 3-4X that of density. This has led to many studies using the ASO data for SWE validation, despite using modeled density [e.g. Broxton *et al.*, 2019; Margulis *et al.*, 2019; Oaida *et al.*, 2019].

### Title change to “Comparison of modeled snow properties in Afghanistan, Pakistan, and Tajikistan”

162-163 Likewise, the success of the Airborne Snow Observatory [Painter *et al.*, 2016] has demonstrated that given accurate depth measurements, SWE can be well modeled.

This makes it difficult to appreciate where the advancement via the new dataset is and whether the point measurements are not lost in the general uncertainty of the satellite data.

The literature review contains all the relevant studies on snow for the region, and as we show, they show wide variation with little to no in situ data used for validation, unlike this study. We therefore suggest that our two take home points discussed below are advancements in snow study for the region.

Additionally I find uncertainties of models inadequately addressed.

We will add a reference about the uncertainty of GLDAS snow estimates.

### 225-229 5.3 Global Data Assimilation System 2 (GLDAS-2)

For comparison, we also include the SWE estimates from GLDAS-2 (Noah). SWE from GLDAS-2 has been shown to be comparable to estimates from other reanalysis datasets, but negatively biased by about 60% in comparison to higher spatial datasets with assimilation from snow station measurements [Broxton *et al.*, 2016].

For the other three models, we do not agree that model uncertainty is not addressed. We refer the referee to previous cited studies on the uncertainties in ParBal [Bair *et al.*, 2016; Rittger *et al.*, 2016] and on modeled SWE from depth in SNOWPACK [Bartelt and Lehning, 2002; Bair *et al.*, 2018a]. On 208-210, we mention the results of Chen *et al.* [2014] who state that NOAA MP was able to model peak SWE in CO USA with a -7% bias.

The stratigraphy is shown as a single mean figure for all stations, with no further consideration of the spatial variability or at least a mention of it and I wonder whether the one line as an aggregate over all station locations does provide a trustworthy result.

Most of the spatial variability is caused by altitude, which is why we show two different plots for the AKAH stations (Figure 9ab) and the higher elevation 25 km pixel containing them (Figure 10ab). The two figures show very different snowpacks.

As a result the Conclusion becomes very brief and somehow lacking the essential take home message for further studies.

We will add to the Conclusion. We will emphasize the two take home messages. 1) ParBal does an accurate job of modeling ablation season SWE at the AKAH stations, validated with in situ measurements; 2) at the coarser 25 km scale, there is wide spread in the SWE across models, with ParBal on the low end.

445-447 Knowledge of the snowpack in northwestern High Mountain Asia is poor. This area is subject to droughts and threatened by snow avalanches. Both problems can be aided by improved knowledge of the snowpack.

455-462 For the models that rely on in situ precipitation measurements, a major challenge is spatial extrapolation, as many of the stations are located in deep valleys. Adding measurements from the mountains above would facilitate more realistic lapse rates, but these measurements do not currently exist, although they would be beneficial both for operational avalanche safety and for scientific studies.

In the regional comparison, SWE estimates from ParBal were on the low end, but given the model spread it is difficult to form a consensus estimate. We plan additional in situ validation at other sites in High Mountain Asia to continue to assess the performance of ParBal there.

And while I appreciate that a number of models were utilized, I think a clearer Figure 2 plus a longer Conclusion on the usefulness of all datasets/models would be prudent.

We will revise Figure 2 to be more clear, per the comments below.

Revised Figure 2

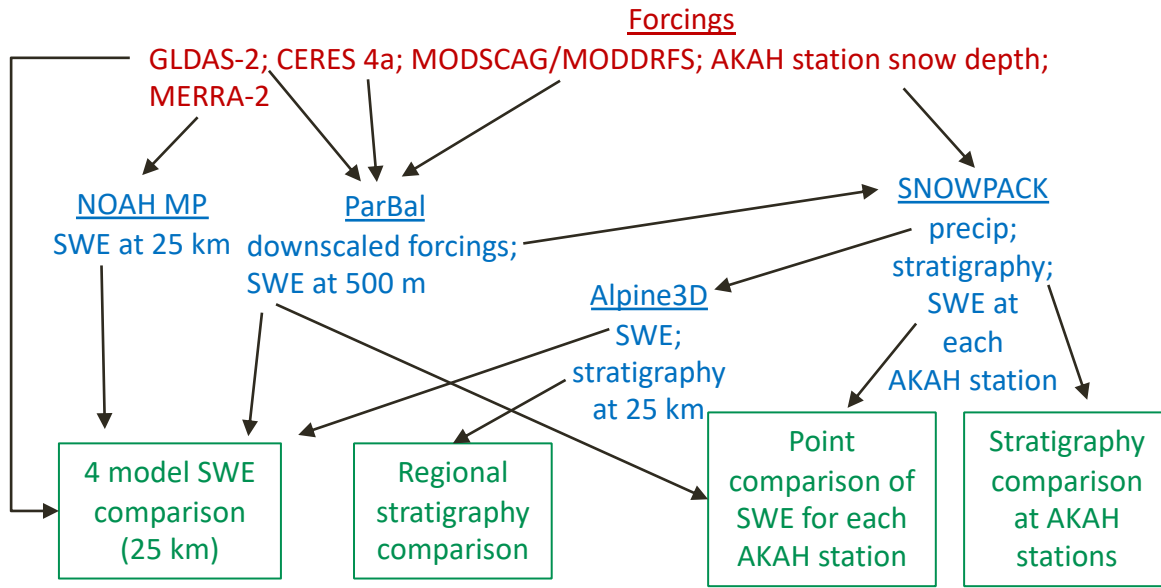


Figure 1 Summary of relationships between the various components. Forcings are shown in red, models and selected outputs are shown in blue, and the comparisons discussed below are shown in green. The black arrows show the direction of inputs.

Minor comments:

Figure 1: Here and in the text (L86) you write 'stations flow into the Indus/Amu Darya'. I get the meaning but I doubt that is technically a sound expression. 'Catchments including stations in xxx drain into the xxx . . .'

Ok, we will correct.

87-88 The rest of the stations in Afghanistan and Tajikistan are in basins that flow into the Amu Darya River.

L93: 'questionable' – although I agree on the assessment, I think you need to explain your criticism rather than just throwing a lead without an argument if you want to mention this here

Ok, we will elaborate.

94-97 For example, the snow and ice albedo is given as 0.20 to 0.30 [Table 3, *Shakoor and Ejaz, 2019*], which would make it 0.10 to 0.20 lower than some of the lowest measured broadband albedo values for dirty snow [*Skiles and Painter, 2016; Bair et al., 2019*].

L103: replace 'x' with 'times' or reword

Ok.

106-107 ...a factor of 2 to 4.

L110: I don't understand how limited climate data would explain why the remotely sensed data from Smith&Bookhagen2018 are too low.

At Salang Pass, Afghanistan, the WMO reports up 198 cm of snow depth [Bair *et al.*, 2018b] and we estimate up to 1000 mm of SWE [Figure S3, Bair *et al.*, 2018b]. Thus < 100 mm of max SWE reported by Smith and Bookhagen is low by up to a factor of 10.

L243: 'hr' to 'hour'

The Cryosphere ([https://www.the-cryosphere.net/for\\_authors/manuscript\\_preparation.html](https://www.the-cryosphere.net/for_authors/manuscript_preparation.html)) requests that SI-accepted units (<https://www.bipm.org/utis/common/pdf/si-brochure/SI-Brochure-9-EN.pdf>) be abbreviated in conjunction with numbers, which would be "h" according to the link above. We'll wait for the Copy Editor to clarify.

L269: the 'Nuristan avalanche' is not a commonly known event. You place a citation later in the text, consider placing that here instead with the description of the impact

Ok

L 305 ...when the Nuristan avalanches took place [United Nations, 2017]

Figure 2: I find the salad of arrows unnecessarily confusing – a number of them could be straight but have corners for no reason making it very hard to decide which path to follow to really get the main aim

Ok, thanks! We were looking for a way to improve the readability.

See revised Figure 2

Figure 7: Remove 'The white letters are . . . codes'. Just the acronyms plus actual names are fine.

Ok.

*Figure 2 Four model (a-d) spatial comparison for the region on 4 May 2018. The white letters are: AFG–Afghanistan; TJK–Tajikistan; and PAK–Pakistan. Also shown in (a) are the locations of the AKAH stations (orange points). This is a frame from a video sequence available as supplementary material.*

Figure 7: The video supplementary material is valuable, however I would also expect a discussion of the consistency/variability between the models in space, i.e. have a corresponding map that shows the average over the complete period or the total number of days the models actually simulate any SWE.

Ok. As the other reviewer pointed out, there are significant differences in snow covered area between the models. We will discuss these differences further. We still find that the video itself is the best way to illustrate these differences, as they vary over space and time.

393-398 For example, the Alpine3D pixels seem to melt out early compared to the other models, especially ParBal, which is the only model relying on satellite-based estimates of fSCA (see



supplementary video). Thus, Alpine3D may be placing too little SWE in cold, high elevation areas that melt slowly. These problems are all indicative of stations that are located in valley bottoms and that only cover the lowest elevations across these 25 km pixels.

Figure 9/10: It is explained in the text but I believe the Figure still needs a y-label

Ok, we will insert a label with "HS/fraction of facets/# of critical layers"

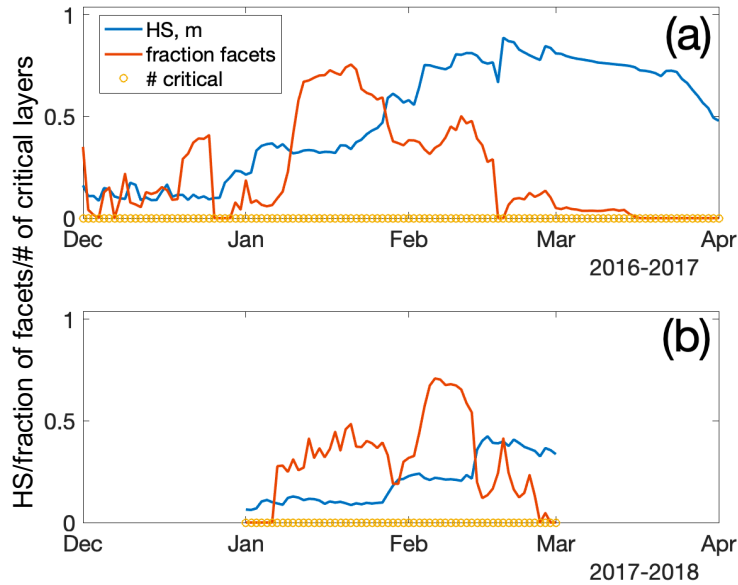


Figure 9 Stratigraphy summary of the AKAH stations for 2017 (a) and 2018 (b). Plotted are the median: height of snow (HS); fraction of the snowpack containing facets; and number of critical layers. The number of stations used to compute the medians varied due to snow coverage.

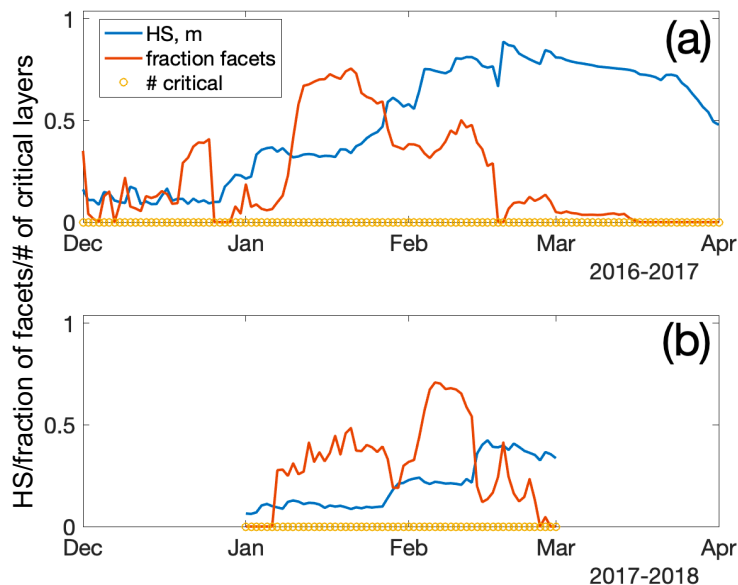


Figure 10 Stratigraphy summary of the AKAH stations for 2017 (a) and 2018 (b). Plotted are the median: height of snow (HS); fraction of the snowpack containing facets; and number of critical layers. The number of stations used to compute the medians varied due to snow coverage.

- Bair, E. H., R. E. Davis, and J. Dozier (2018a), Hourly mass and snow energy balance measurements from Mammoth Mountain, CA USA, 2011–2017, *Earth Syst. Sci. Data*, 10(1), 549-563, doi: 10.5194/essd-10-549-2018.
- Bair, E. H., A. Abreu Calfa, K. Rittger, and J. Dozier (2018b), Using machine learning for real-time estimates of snow water equivalent in the watersheds of Afghanistan, *The Cryosphere*, 12(5), 1579-1594, doi: 10.5194/tc-12-1579-2018.
- Bair, E. H., K. Rittger, S. M. Skiles, and J. Dozier (2019), An Examination of Snow Albedo Estimates From MODIS and Their Impact on Snow Water Equivalent Reconstruction, *Water Resources Research*, 55(9), 7826-7842, doi: 10.1029/2019wr024810.
- Bair, E. H., K. Rittger, R. E. Davis, T. H. Painter, and J. Dozier (2016), Validating reconstruction of snow water equivalent in California's Sierra Nevada using measurements from the NASA Airborne Snow Observatory, *Water Resources Research*, 52, 8437-8460, doi: 10.1002/2016WR018704.
- Bartelt, P., and M. Lehning (2002), A physical SNOWPACK model for the Swiss avalanche warning: Part I: numerical model, *Cold Regions Science and Technology*, 35(3), 123-145, doi: 10.1016/s0165-232x(02)00074-5.
- Broxton, P. D., X. Zeng, and N. Dawson (2016), Why Do Global Reanalyses and Land Data Assimilation Products Underestimate Snow Water Equivalent?, *J. Hydrometeorol.*, 17(11), 2743-2761, doi: 10.1175/jhm-d-16-0056.1.
- Broxton, P. D., W. J. D. van Leeuwen, and J. A. Biederman (2019), Improving Snow Water Equivalent Maps With Machine Learning of Snow Survey and Lidar Measurements, *Water Resources Research*, 55(5), 3739-3757, doi: 10.1029/2018wr024146.
- Chen, F., et al. (2014), Modeling seasonal snowpack evolution in the complex terrain and forested Colorado Headwaters region: A model intercomparison study, *Journal of*

- Geophysical Research: Atmospheres, 119(24), 13,795-713,819, doi: 10.1002/2014jd022167.
- Margulis, S. A., Y. Fang, D. Li, D. P. Lettenmaier, and K. Andreadis (2019), The Utility of Infrequent Snow Depth Images for Deriving Continuous Space-Time Estimates of Seasonal Snow Water Equivalent, *Geophysical Research Letters*, 46(10), 5331-5340, doi: 10.1029/2019gl082507.
- Marks, D., and J. Dozier (1992), Climate and energy exchange at the snow surface in the alpine region of the Sierra Nevada, 2, Snow cover energy balance, *Water Resources Research*, 28(11), 3043-3054, doi: 10.1029/92WR01483.
- Oaida, C. M., J. T. Reager, K. M. Andreadis, C. H. David, S. R. Levoe, T. H. Painter, K. J. Bormann, A. R. Trangsrud, M. Giroto, and J. S. Famiglietti (2019), A High-Resolution Data Assimilation Framework for Snow Water Equivalent Estimation across the Western United States and Validation with the Airborne Snow Observatory, *J. Hydrometeorol.*, 20(3), 357-378, doi: 10.1175/jhm-d-18-0009.1.
- Painter, T. H., et al. (2016), The Airborne Snow Observatory: Fusion of scanning lidar, imaging spectrometer, and physically-based modeling for mapping snow water equivalent and snow albedo, *Remote Sensing of Environment*, 184, 139-152, doi: 10.1016/j.rse.2016.06.018.
- Rittger, K., E. H. Bair, A. Kahl, and J. Dozier (2016), Spatial estimates of snow water equivalent from reconstruction, *Advances in Water Resources*, 94, 345-363, doi: 10.1016/j.advwatres.2016.05.015.
- Shakoor, A., and N. Ejaz (2019), Flow Analysis at the Snow Covered High Altitude Catchment via Distributed Energy Balance Modeling, *Scientific Reports*, 9(1), 4783, doi: 10.1038/s41598-019-39446-1.
- Skiles, S. M., and T. Painter (2016), Daily evolution in dust and black carbon content, snow grain size, and snow albedo during snowmelt, Rocky Mountains, Colorado, *Journal of Glaciology*, 63(237), 118-132, doi: 10.1017/jog.2016.125.
- United Nations (2017), Afghanistan: Nuristan avalanche, update to flash report (as of 8 February 2017)Rep., Office for the Coordination of Humanitarian Affairs (OCHA).

1 **Comparison of modeled snow properties in Afghanistan, Pakistan, and Tajikistan**

Deleted: Validation of

2  
3 Edward H. Bair<sup>1</sup>, Karl Rittger<sup>2</sup>, Jawairia A. Ahmad<sup>3</sup>, and Doug Chabot<sup>4</sup>

4  
5 <sup>1</sup>Earth Research Institute, University of California, Santa Barbara, California, USA  
6 6832 Ellison Hall, University of California, Santa Barbara, CA 93106-3060. correspondence  
7 email: nbair@eri.ucsb.edu

8  
9 <sup>2</sup>Institute for Arctic and Alpine Research, University of Colorado, Boulder, Colorado, USA

10  
11 <sup>3</sup>Department of Civil & Environmental Engineering, University of Maryland, College Park, MD,  
12 USA

13  
14 <sup>4</sup>independent researcher, Bozeman, MT, USA

16 ABSTRACT: Ice and snowmelt feed the Indus and Amu Darya rivers, yet there are limited in situ  
17 measurements of these resources. Previous work in the region has shown promise using snow  
18 water equivalent (SWE) reconstruction, which requires no in situ measurements, but validation  
19 has been a problem until recently when we were provided with daily manual snow depth  
20 measurements from Afghanistan, Tajikistan, and Pakistan by the Aga Khan Agency for Habitat  
21 (AKAH). For each station, accumulated precipitation and SWE were derived from snow depth  
22 using the SNOWPACK model. High-resolution (500 m) reconstructed SWE estimates from the  
23 ParBal model were then compared to the modeled SWE at the stations. The Alpine3D model was  
24 then used to create spatial estimates at 25 km to compare with estimates from other snow models.  
25 Additionally, the coupled SNOWPACK and Alpine3D system has the advantage of simulating  
26 snow profiles, which provide stability information. Following previous work, the median number  
27 of critical layers and percentage of facets across all of the pixels containing the AKAH stations  
28 was computed. For SWE at the point scale, the reconstructed estimates showed a bias of -42 mm  
29 (-19%) at the peak. For the coarser spatial SWE estimates, the various models showed a wide  
30 range, with reconstruction being on the lower end. For stratigraphy, a heavily faceted snowpack is  
31 observed in both years, but 2018, a dry year, according to most of the models, showed more critical  
32 layers that persisted for a longer period.

33 1 INTRODUCTION

34 There are many parts of the world where little is known about the snowpack. This lack of  
35 knowledge presents a challenge for water managers and for avalanche forecasters. Afghanistan is  
36 particularly austere in this respect, as there have been no snow measurements available since the  
37 early 1980s. This lack of information about the snowpack potentially creates a humanitarian crisis,  
38 as snowmelt fed streams run dry in the fall without warning (USAID, 2008). Accurate historical  
39 estimates of basin-wide snow water equivalent (SWE) are crucial for creating a baseline of  
40 climatological conditions, which can then aid in predicting today’s SWE. For example,  
41 climatological estimates of spatially-distributed SWE are the most important predictors in machine  
42 learning statistical models for this region (Bair et al., 2018b).

43 To improve our knowledge about the snowpack in these areas, we have developed an approach  
44 that requires no in situ measurements. Using satellite-based estimates of the fractional snow-  
45 covered area (fSCA) and downscaled forcings in an energy balance model, we build up the  
46 snowpack in reverse, from melt out to its peak, using a technique called SWE reconstruction  
47 (Martinec and Rango, 1981). This technique has been shown to accurately estimate SWE in  
48 mountain ranges across the world, including: the Sierra Nevada USA (Bair et al., 2016; Rittger et  
49 al., 2016); the Rocky Mountains USA (Jepsen et al., 2012; Molotch, 2009); and the Andes of South  
50 America (Cornwell et al., 2016)—all areas with relatively abundant independent ground validation  
51 measurements. For the so called Third Pole of High Mountain Asia, and especially the  
52 northwestern parts of this region, e.g. Afghanistan, Tajikistan, and Pakistan, ground-based  
53 validation is challenging.

54 2 AGA KHAN AGENCY FOR HABITAT (AKAH) STATIONS

55 In 2017, we received daily manual snow depth and other meteorological measurements from  
56 nearly 100 stations (Figure 1) in an operational avalanche network (Chabot and Kaba, 2016). These  
57 stations are funded by the Aga Khan Agency for Habitat (AKAH) and are the first snowpack  
58 measurements available, at least that we are aware of, in Afghanistan in nearly 40 years. Hence,  
59 we refer to the region as the AKAH study region and the weather stations as the AKAH stations.  
60 The AKAH stations contain manual daily snow depth (also called height of snow), height of new  
61 (24-hr) snow, daily high and low air temperature, instantaneous wind speed/direction, rainfall, and  
62 some text fields on weather and avalanche conditions. For mountainous areas, precipitation is the  
63 most uncertain term in the water balance (Adam et al., 2006; Milly and Dunne, 2002) because it  
64 exhibits high spatial variability and is difficult to measure with traditional gauges. Measuring snow  
65 on the ground has many advantages compared to using precipitation gauges, which suffer from  
66 undercatch, especially in the windy and treeless areas (Goodison et al., 1998; Kochendorfer et al.,  
67 2017; Lehning et al., 2002a) typical of this part of the world. Likewise, a strength of the SWE  
68 reconstruction technique is that it does not depend on precipitation measurements to build the  
69 snowpack.

70 Additionally, many of the AKAH stations are at high altitudes, with 64 stations above 2500 m and  
71 17 stations above 3000 m. Unfortunately, most of these stations are located in deep valleys, where  
72 the villages are, rather than on exposed mountain sides or ridges and the daily resolution is too  
73 coarse to use in a snow model without temporal interpolation. Additionally, many of the stations  
74 are near glacierized areas which complicates spatially interpolated snow estimates, as some of the  
75 snow is on top of ice. The area covered by glaciers in Figure 1 is 7.8%.



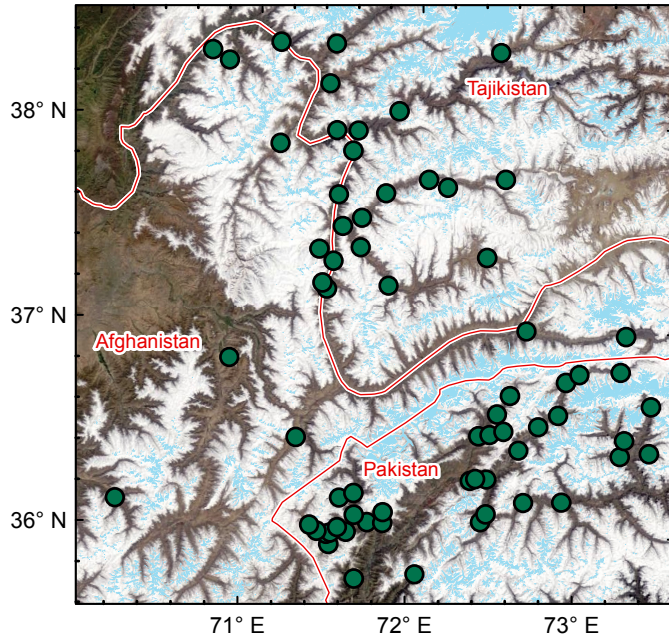


Figure 1 Study region with AKAH stations (green dots) overlaid on a MODIS true color image from 13 April 2018. Also shown are the country boundaries (red) and glacierized areas (light blue) from the Global Land Ice Measurement from Space dataset (Raup et al., 2007). All of the stations in Afghanistan and Tajikistan eventually flow into the Amu Darya River. All of the stations in Pakistan eventually flow into the Indus River.

76

77 Although there have been a large number of studies examining the glaciers of High Mountain Asia,  
 78 there are fewer studies examining snowfall in High Mountain Asia, which is odd since  
 79 hydrologically in this region, snow on land melt provides the vast majority of runoff compared to  
 80 snow on ice and melting glacier ice (Armstrong et al., 2018). Many of these studies are focused on  
 81 the region to the east of the AKAH study area shown in Figure 1. To our knowledge, there have  
 82 been no studies on snowpack stratigraphy in the AKAH study area and we were unable to obtain  
 83 any snow pit measurements from this area.

### 84 3 LITERATURE REVIEW

85 A few studies have specifically examined snowfall in larger regions that include some of the  
 86 AKAH stations, mostly for stations in the southern basins that flow into the Indus River; that is all  
 87 of the stations in Pakistan. The rest of the stations in Afghanistan and Tajikistan are in basins that  
 88 flow into the Amu Darya River. The most comparable study (Shakoor and Ejaz, 2019) examines  
 89 the Passu catchment in the Hunza River Basin, to the east of Figure 1. As in this study (Section  
 90 5.1), Shakoor and Ejaz (2019) also use the SNOWPACK and Alpine3D models. Model parameters  
 91 were calibrated using a single weather station, Urdukas at 3926 m elevation near the Baltoro glacier

92 (Ev-K2-CNR, 2014), with one year of precipitation measurements, using snow depth for  
93 validation. The authors report overestimation of the measured snow depth at the calibration station,  
94 even after questionable adjustments to the snow albedo and other model parameters. For example,  
95 the snow and ice albedo is given as 0.20 to 0.30 (Table 3, Shakoor and Ejaz, 2019), which would  
96 make it 0.10 to 0.20 lower than some of the lowest measured broadband albedo values for dirty  
97 snow (Bair et al., 2019; Skiles and Painter, 2016). They attribute the overestimation to problems  
98 with the precipitation measurements, common for high altitude stations. One problem with the  
99 Urdukas station in particular is that the tipping bucket precipitation gauge is unheated, making it  
100 unusable for measuring solid precipitation. Temperatures at this station were well below freezing  
101 for the winter and most of the spring, which explains why no precipitation was recorded from  
102 January until sometime in March during 2012, the calibration year.

Deleted:

103 Viste and Sorteberg (2015) study several gridded precipitation products throughout High Mountain  
104 Asia, including the Indus River Basin. They report that while total precipitation was similar across  
105 the products—including MERRA (Rienecker et al., 2011), APHRODITE (Yatagai et al., 2012),  
106 TRMM (Huffman et al., 2007), and CRU (Harris et al., 2014)—the total snowfall varied by a factor  
107 of 2 to 4. Smith and Bookhagen (2018) used 24 years (1987 to 2009) of satellite-based passive  
108 microwave SWE estimates to examine trends throughout High Mountain Asia, including the Amu  
109 Darya and Indus Basins. Their SWE estimates show most 25 km pixels in this region in the 50-  
110 100 mm range for December through February, with a few over 100 mm in the Amu Darya (i.e.  
111 all the AKAH stations in Afghanistan and Tajikistan) and none over 100 mm in the Indus (i.e. all  
112 the AKAH stations in Pakistan), likely too low by an order of magnitude for some pixels given our  
113 previous reconstructed SWE values and limited climate measurements in Afghanistan (Bair et al.,  
114 2018b).

Deleted: 2 to 4 ×

115 For the AKAH stations in Tajikistan, the most comprehensive snow measurements come from  
116 Soviet snow surveys (mostly depth, but with some SWE and density measurements) that have been  
117 digitized (Bedford and Tsarev, 2001). Most of these measurements begin in the late 1950s and end  
118 around the fall of the Soviet Union, in either 1990 or 1992, making them useful for climatological  
119 studies, but not for validation of modern satellite-based estimates.

120 The sole source of snow measurements in Afghanistan that were accessible to us was a table of  
121 outdated WMO monthly climatological data from Kabul (el. 1791 m) and North Salang (el. 3366  
122 m), showing the maximum monthly snow depth and the mean number of days with snow (Table 1  
123 in Bair et al., 2018b). Again, these measurements are not useful to validate more modern snow  
124 estimates.

125 There have been many other studies that have attempted to estimate basin-wide precipitation  
126 (including snowfall) for larger areas that include the AKAH region, especially in the Indus. Several  
127 climate studies of the Indus have focused on using lower elevation precipitation gauges, which are  
128 then used to spatially interpolate basin-wide precipitation. Dahri et al. (2016) and Dahri et al.  
129 (2018) have assembled perhaps the largest collection of climatological measurements covering the  
130 AKAH region, mostly based on gauge measurements, as part of a study on the hydrometeorology  
131 of the Indus Basin. Using undercatch corrections based on wind, often from reanalysis, they  
132 increased precipitation estimates by 21% on average throughout the Indus Basin (Dahri et al.,  
133 2018). For example, in the Gilgit sub-basin, they find an unadjusted precipitation estimate of 582  
134 mm/year, adjusted to 787 mm/year, a 35% increase. Although some of the measurements are taken  
135 from publicly available sources, as with most publications for this region, the comprehensive data  
136 used are not publicly accessible.

139 A similar but less sophisticated approach was used by Lutz et al. (2014), who used a constant  
140 increase of 17% across the APHRODITE precipitation dataset which covers all of High Mountain  
141 Asia. Immerzeel et al. (2015) used glacier mass balance estimates with streamflow measurements  
142 as validation to show that high-altitude precipitation in the upper Indus Basin is 2 to 10 × what is  
143 shown using gridded precipitation products like APHRODITE. Bookhagen and Burbank (2010)  
144 estimate that snowmelt contributes 66% of annual discharge to the Indus, and averages 424 mm  
145 across the basin.

146 In summary, quite a few studies have produced varying precipitation and snowfall estimates for  
147 the AKAH region, with no recent in situ snow measurements from Afghanistan or Tajikistan.

#### 148 4 PREVIOUS WORK WITH AKAH SNOW MEASUREMENTS

149 Our previous work (Bair et al., 2018b) used a simple density model (Sturm et al., 2010) based on  
150 snow climatology (Sturm et al., 1995) and day of year to model SWE from the manual snow depth  
151 measurements. The density model itself has -12 to 26% bias in predicting SWE. When taking into  
152 account geolocational uncertainty of the reconstructed SWE estimates and uncertainty in the  
153 density model, errors are on the order of 11-13% Mean Absolute Error (MAE) and -2 to 4% bias,  
154 depending on the date. However, we only examined one year of the AKAH station data (2017)  
155 and the high uncertainty in the density model itself begs a more sophisticated approach.

156 From recent work (Bair et al., 2018a), we have shown that the SNOWPACK (Bartelt and Lehning,  
157 2002; Lehning et al., 2002a; Lehning et al., 2002b) model is capable of accurate SWE prediction  
158 when supplied only with snow depth for precipitation, as well as the other requisite forcings (i.e.  
159 radiation, snow albedo, temperatures, and wind speed). Over a 5-year period using hourly in situ  
160 measured energy balance forcings and a snow pillow for validation at a high elevation site in the  
161 western US, the SNOWPACK modeled SWE showed a bias of -17 mm or 1% (Bair et al., 2018a).  
162 Likewise, the success of the Airborne Snow Observatory (Painter et al., 2016) has demonstrated  
163 that given accurate depth measurements, SWE can be well modeled.

#### 164 5 METHODS

165 Our modeling approach consisted of: a) downscaling forcings in ParBal and reconstructing SWE;  
166 b) combining the downscaled forcings for each AKAH station with temporally interpolated manual  
167 snow measurements; c) running SNOWPACK for each of the AKAH stations with the downscaled  
168 and interpolated measurements from a) and b); and d) running Alpine3D using the output from  
169 SNOWPACK, notably the hourly precipitation. In addition to predicting SWE, the  
170 SNOWPACK/Alpine3D coupled model also predicts stratigraphic parameters useful for avalanche  
171 prediction, thereby giving us an idea of the layering and stability in this region. For comparison,  
172 we also ran the NOAA-MP land surface model over the region with widely-used forcings. We also  
173 compared spatial estimates of SWE from GLDAS-2. Methods are summarized in Table 1 and  
174 explained below, with more detail provided in Appendix A.

##### 175 5.1 SNOWPACK and Alpine3D

176 SNOWPACK and Alpine3D are freely available (<https://models.slf.ch>) point and spatially  
177 distributed snow models, courtesy of the Swiss Federal Snow Institute. SNOWPACK is the older  
178 of the two and uses finite elements to model all of the layers in a snowpack at a point.

Deleted: (Yatagai et al., 2012)

Model	Point comparison?	Spatial comparison?	Version	Forcings	Output
ParBal	√	√	1.0	CERES 4a (radiation); GLDAS-2 (meteorological); MODSCAG/MODDRFS (snow surface properties)	Daily reconstructed SWE at 500 m; hourly downscaled forcings at 500 m, both for entire AKAH study area
SNOWPACK	√		3.5	AKAH station snow measurements; downscaled forcings from ParBal	Hourly SWE, precipitation, and other forcings for each AKAH station
Alpine3D		√	3.1	AKAH station output from SNOWPACK	Daily SWE at 25 km for entire AKAH study area
NOAH MP		√	3.6	MERRA-2	Daily SWE at 25 km for entire AKAH study area
GLDAS		√	NOAH 2.1	various	Daily SWE at 25 km for entire AKAH study area

180 *Table 1 Summary of models used. See Section 5 and Appendix A for an explanation of acronyms and further*  
181 *details.*

182 SNOWPACK has shown promising results in both operational (e.g. Lehning et al., 1999;  
183 Nishimura et al., 2005) and research applications (e.g. Bellaire et al., 2011; Hirashima et al., 2010).  
184 Previous results with SNOWPACK (Bair et al., 2018a) show high model sensitivity to  
185 precipitation, but only a 1% error in modeled SWE when using snow depth only (not total  
186 precipitation) as a forcing. Thus, given reliable snow depth measurements at each AKAH station  
187 (see Section 5.5), modeled SWE during the accumulation season is treated as having negligible  
188 uncertainty. During the ablation season (after peak SWE), uncertainty is higher. Unlike during  
189 snow accumulation events, SNOWPACK does not force its modeled snow ablation to match the  
190 measured snow depth decreases. Uncertainty in SWE during the ablation season is then largely  
191 dependent on radiative forcings (Marks and Dozier, 1992) and the broadband snow albedo (Bair  
192 et al., 2019). Here, 5% uncertainty is used, based on the MAE from SWE reconstructions using  
193 the same remotely-sensed forcings at a continental sub-alpine site (Bair et al., 2019). In the same  
194 study, a small (3%) bias in SWE was also found, but this is likely due to shortcomings with the  
195 reconstruction method and not applicable to SWE modeled with SNOWPACK. Thus, the small  
196 bias was ignored. We acknowledge that these uncertainty estimates are themselves uncertain, e.g.

197 [the reanalysis forcings could be especially poor for this region compared to those available in the](#)  
198 [western US.](#)

199 Alpine3D (Lehning et al., 2006) is essentially a spatially-distributed version of SNOWPACK with  
200 a number of additional modules including: terrain-based radiation modeling, blowing snow, and  
201 hydrologic modeling. Integral to Alpine3D is SNOWPACK, which is run for each pixel, as well  
202 as the MeteorIO library (Bavay and Egger, 2014), which provides a large number of temporal and  
203 spatial interpolation functions that can be used on forcings for Alpine3D and SNOWPACK.

## 204 5.2 The Parallel Energy Balance Model

205 The Parallel Energy Balance Model (ParBal) was created at UC-Santa Barbara and designed for  
206 reconstruction of SWE. It is also publicly available  
207 (<https://github.com/edwardbair/ParBal/releases/tag/v1.0>). Currently, ParBal is designed to use:  
208 downscaled temperature, pressure, and humidity from version 2 of the Global or National Land  
209 Data Assimilation System (GLDAS-2/NLDAS-2, Rodell et al., 2004; Xia et al., 2012); shortwave  
210 and longwave radiation from edition 4a of the Clouds and the Earth's Radiant Energy System  
211 (CERES, Rutan et al., 2015) SYN product; and time-spaced smoothed (Dozier et al., 2008; Rittger  
212 et al., in press) snow surface properties from MODIS Snow Covered Area and Grain Size  
213 (MODSCAG, Painter et al., 2009) and MODIS Dust and Radiative Forcing in Snow (MODDRFS,  
214 Painter et al., 2012). ParBal is run hourly at 500 m spatial resolution and forcings are adjusted for  
215 terrain and elevation. The main output is the residual energy balance term, which is assumed to go  
216 into melt when positive during the ablation phase after cold content is overcome (Jepsen et al.,  
217 2012). This residual melt term is then summed in reverse during periods of contiguous snow cover  
218 and multiplied by the fSCA to spread the snow spatially. [The errors in SWE from ParBal are](#)  
219 [mostly from fSCA and the radiative forcings. Errors and details on ParBal are covered extensively](#)  
220 [in Bair et al. \(2016\) and Rittger et al. \(2016\). In the supplement for Bair et al. \(2018b\), the errors](#)  
221 [arising from using GLDAS-2 and CERES 4a \(available worldwide but at coarser spatial resolution\)](#)  
222 [vs. NLDAS-2 are specifically evaluated. Using three years of basin-wide SWE estimated by the](#)  
223 [Airborne Snow Observatory in the upper Tuolumne Basin, California USA, the MAE for ParBal](#)  
224 [was 25 mm or 26% \(Bair et al., 2018b\).](#)

## 225 5.3 Global Data Assimilation System 2 (GLDAS-2)

226 [For comparison, we also include the SWE estimates from GLDAS-2 \(Noah\). SWE from GLDAS-](#)  
227 [2 has been shown to be comparable to estimates from other reanalysis datasets, but negatively](#)  
228 [biased by about 60% in comparison to higher spatial datasets with assimilation from snow station](#)  
229 [measurements \(Broxton et al., 2016\).](#)

## 230 5.4 NOAA Multi-Parameterization (MP)

231 The NOAA-MP v3.6 (Ek et al., 2003; Niu et al., 2011) land surface model, forced using MERRA-  
232 2 (Gelaro et al., 2017), was used to simulate the hydrologic cycle over the study area and provide  
233 SWE estimates for comparison with ParBal and the Alpine3D output. NOAA-MP was selected  
234 due to its detailed representation of the snowpack relative to other land surface models. The model  
235 subdivides the snowpack into up to three layers with associated liquid water storage and  
236 melt/refreeze capability (Niu and Yang, 2004; Yang and Niu, 2003). It incorporates the exchange  
237 of heat and moisture through the snowpack between the land surface and the atmosphere. In a

Deleted: Details on

Deleted: .

Deleted: (Bair et al., 2018b)

Formatted: Heading 3

241 model intercomparison study using a 2 km spatial resolution regional climate model for forcings,  
242 Chen et al. (2014) show that NOAA-MP modeled peak SWE at SNOTEL sites in Colorado, USA  
243 with a -7% bias.

#### 244 5.5 *Use of AKAH station measurements*

245 We modeled daily SWE at the AKAH stations during the 2017 and 2018 water years primarily  
246 using the manually measured height of snow (HS), also called snow depth, combined with our  
247 downscaled energy balance parameters (for downscaling methodology see Bair et al., 2018b; Bair  
248 et al., 2016; Rittger et al., 2016). To our knowledge, no quality control was performed on the  
249 AKAH station measurements before we received them. We choose the manual HS and new (24-  
250 hr) snow (HN) as the only variables to use from the AKAH stations. The HS appeared to be the  
251 most reliably measured, as that only requires reading a value from a master snow depth stake.  
252 Apart from spurious drops or missing values (see below), the HS measurement appeared consistent  
253 and believable at most of the stations, implying an accurate snow depth record. The HN was used  
254 to correct a data entry problem in 2017 that we discuss below. The reliability of the other  
255 measurements (instantaneous wind speed/direction, maximum/minimum temperature, and  
256 rainfall) was questionable. For example, we were not provided with sensor or measurement  
257 metadata, e.g. sensor make/model, measurement height, and whether or not the temperature sensor  
258 was shielded from shortwave radiation. These other measurements taken daily were also of limited  
259 value for interpolation to hourly values (see item 3 below). Thus, these other measurements were  
260 not used.

261 The AKAH dataset had a number of shortcomings that we list here along with how we addressed  
262 them.

- 263 1) Some of the stations recorded no snow at all, especially in the dry 2018 year, or had obvious  
264 problems, such as weeks of missing measurements, so they were excluded. For 2017, 52 (54%)  
265 of stations were used. For 2018, 41 (46%) stations were used.
- 266 2) There were spurious drops in the HS measurements. The drops were clearly cases of missing  
267 values being filled with zeros. These measurements were manually flagged and converted to  
268 null values for interpolation, see below.
- 269 3) The daily measurements had to be interpolated to hourly values. For the most part we used  
270 linear interpolation, although this is not ideal during snow accumulation since it's almost never  
271 the case that snowfall is uniform over a 24-hr period. This is a problem that affects the accuracy  
272 of snow settlement estimated by SNOWPACK. There were two cases where other interpolation  
273 methods were used. If there were several days of missing values, we used a nearest neighbor  
274 interpolation to fill in the missing daily values, followed by a linear interpolation from daily to  
275 hourly measurements such that we assumed all the new snow fell in a 24-hr period. The other  
276 case was for days where the linear interpolation would yield a value below the minimum  
277 threshold hard coded into SNOWPACK (0.5cm/hr) for the first accumulating snowfall on bare  
278 ground. In this case, a previous neighbor interpolation was used in such a way that the entire  
279 snowfall occurred in the last hr prior to the next day's measurement.
- 280 4) We found the AKAH stations suitable for snow on the ground measurements, but not for  
281 rainfall or total (solid+liquid) precipitation. This was only an issue for the Alpine3D snow  
282 modeling, as snow measurements were being extrapolated to higher elevations than the AKAH

Deleted: <#>¶

Deleted:



285 stations (Section 6.2), thus at these higher elevations, snow accumulated earlier and melted  
286 later than at the lower AKAH stations.

287 Given the near total lack of canopy cover in the region, we suspected substantial undercatch from  
288 rain gauges. Using the wind speed, an undercatch correction would have been possible given more  
289 information on the gauges (e.g. orifice opening diameter and whether or not a shield was present),  
290 however this instrument metadata was not available to us. Likewise, we did not know if the gauges  
291 were heated or not.

292 Further, the time period for recording measurements from the stations was not consistent. In WY  
293 2017, measurements began being reported on 10 November 2016 and were reported until 24  
294 November 2017. However, in WY 2018, measurements weren't reported until 1 December 2017  
295 and no station measurements were reported past 1 April 2017. The reporting period likely covered  
296 all the snowfall events, but not all the precipitation events.

297 To address the rainfall measurement and reporting issues, we used GLDAS NOAH v2.1 (Rodell  
298 et al., 2004) rainfall + snowfall from the nearest grid cell (1/4° spatial / 3 hr temporal resolution)  
299 to fill in precipitation prior to the first measurements in each water year, and after 4-1 for both  
300 water years. We did not account for rain from 10 November 2016 to 1 April 2017 and from 1  
301 December 2017 to 1 April 2018; instead we relied on the modeled precipitation from SNOWPACK  
302 using snow depth. The AKAH station observations show that rain during this time period was rare.

303 5) A database problem prevented snow heights > 100 cm from being entered into the database for  
304 a few days in 2017. This problem became apparent during February 2017, when the Nuristan  
305 avalanches took place ([United Nations, 2017](#)), as that is the first time that most stations  
306 recorded values > 100 cm. Values were shown as 100 cm on multiple days followed by values  
307 > 100 cm. To address this issue, we flagged all the values equal to 100 cm prior to peak depth  
308 in 2017, then marked those as null values. We then filled those null values using the cumulative  
309 sum of new snow during that time.

### 310 5.6 Analysis of modeled snow profiles

311 For holistic measures of the snow profiles modeled in Alpine3D, we used two metrics from  
312 Bellaire et al. (2018): 1) fraction of facets and 2) number of critical layers. Fraction of facets is the  
313 height of all the layers containing faceted crystals, i.e. International Classification for Seasonal  
314 Snow on the Ground primary codes FC, DH, and SH (Fierz et al., 2009), divided by the height of  
315 the snowpack. The number of critical layers was computed using a threshold sum approach  
316 (Schweizer and Jamieson, 2007) with modifications for simulated profiles (Monti et al., 2014  
317 Table 1). In each profile, 6 different variables (grain size, difference in grain size, hardness,  
318 difference in hardness, grain type, and depth) in the top meter of height (from the surface) were  
319 checked against threshold values. Layers exceeding 5 or more thresholds were classified as critical.

320 The fraction of facets metric does not have a validation study, but faceted layers are a weak crystal  
321 form and are responsible for 43% (Bair et al., 2012) to 67% (Schweizer and Jamieson, 2001) of  
322 investigated avalanches. Layers classified as critical using the threshold approach above  
323 corresponded to failure layers about ½ of the time (Monti et al., 2014) in Compression Tests  
324 (Jamieson, 1999; van Herwijnen and Jamieson, 2007), an in situ snowpack stability test.

325 5.7 Spatial scale for comparisons

326 Because ParBal is the only model run at 500 m spatial resolution and all the other models were run  
 327 at ~ 25 km, it is the only model appropriate for point comparisons, although point to area problems  
 328 are still an issue. To address the geolocational uncertainty for the gridded MODIS products, which  
 329 can be up to one ~500 m pixel (Tan et al., 2006; Xiaoxiong et al., 2005) and spatial variability of  
 330 the snow, we used a 9-pixel neighborhood centered on each AKAH station and chose the best fit  
 331 to the SNOWPACK modeled SWE. This approach has been used in previous work (Bair et al.,  
 332 2018b; Rittger et al., 2016). We also include the high and low SWE values in that surrounding 9-  
 333 pixel neighborhood to bound the uncertainty.

334 For all of the other model comparisons, we resampled all of the model output to a UTM (Zone  
 335 43S) grid with 25 km pixels, close to the native resolution of the NOAA-MP and GLDAS2 grid  
 336 used (0.25°). The ParBal output had to be significantly upscaled from 500 m to 25 km using  
 337 Gaussian Pyramid reduction (Burt and Adelson, 1983) in steps with bilinear interpolation for the  
 338 final step.

339 6 RESULTS AND DISCUSSION

340 The relationships between the components are summarized in Figure 2. The results discussed  
 341 below are comparisons of: 1) SWE and 2) snow stratigraphy across a) all of the AKAH stations  
 342 (points) and b) the entire study region.

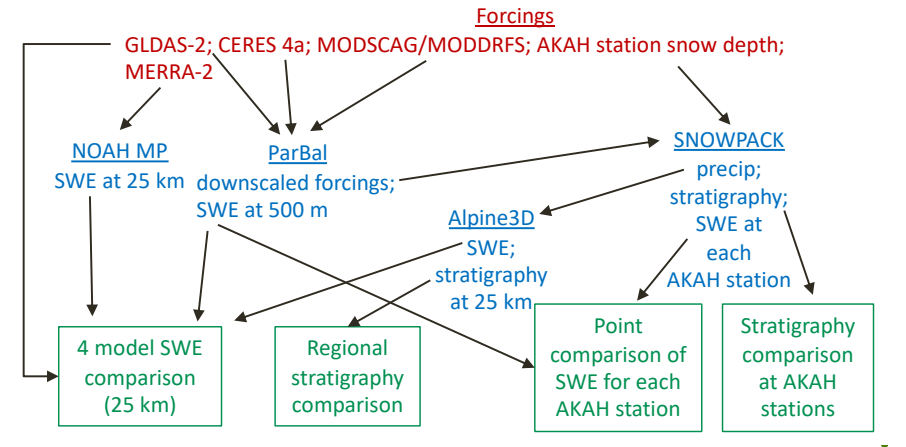
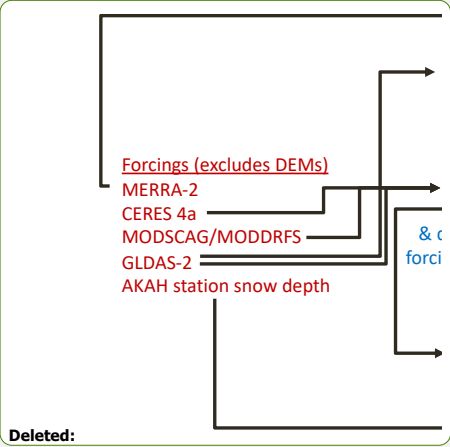


Figure 2 Summary of relationships between the various components. Forcings are shown in red, models and selected outputs are shown in blue, and the comparisons discussed below are shown in green. The black arrows show the direction of inputs.

343

344 6.1 Point comparisons between SNOWPACK and reconstructed SWE

345 A first step for any SWE reconstruction comparison is to determine when the ablation season starts.  
 346 This varies for different years and at different sites (e.g. Margulis et al., 2016). Using the



347 SNOWPACK modeled SWE, we can examine the peak SWE dates for both years for all of the  
 348 AKAH stations (Figure 3ab). Peak SWE dates vary across the stations and years, but the median  
 349 values between years are a week apart, 19 February 2017 and 26 February 2018. Thus, we use  
 350 those dates for our comparisons.

Deleted: are

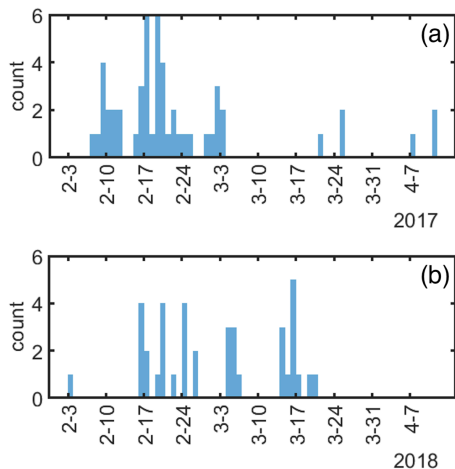


Figure 3 Peak SWE dates, modeled by SNOWPACK for 2017 (a) and 2018 (b) for each of the AKAH stations. The median peak SWE dates are 19 February 2017 and 26 February 2018. N=52 and 41 AKAH stations used for 2017 and 2018.

351  
 352 To create a holistic comparison for all the stations across the ablation period, mean SWE values  
 353 were computed and plotted for each day during the ablation season (Figure 4). For the  
 354 reconstructed SWE on 19 February 2017, the bias is -77 mm (-28%). For the reconstructed SWE  
 355 on 26 February 2018, the bias is -6 mm (-9%). Thus, together these biases average to -42 mm (-  
 356 19%). The high/low values in the 9-pixel neighborhood show the wide spatial variation in SWE  
 357 estimates, and are to be expected in these deep valley sites (Section 6.2). The increases in  
 358 reconstructed SWE during the ablation season are caused due to differences in how melt is summed  
 359 for any given pixel. In ParBal, melt is only summed during periods of contiguous snow cover. This  
 360 means that if a pixel containing an AKAH station has no snow on it at some point during the  
 361 ablation season, but then snow is detected, it causes an increase in the mean SWE. This is called  
 362 an ephemeral snow event, i.e. snow that disappears and reappears. For a more in depth examination  
 363 of the error at individual stations, a box plot is shown for the median peak SWE dates for both  
 364 years (Figure 5). The median bias of the reconstructed SWE is -11 mm (-14%).

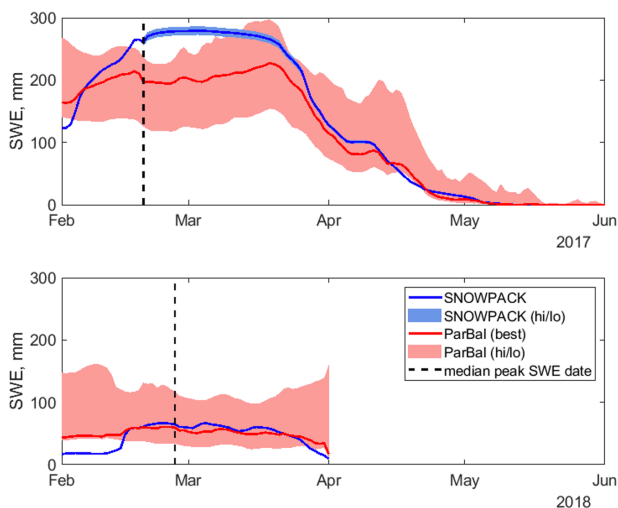
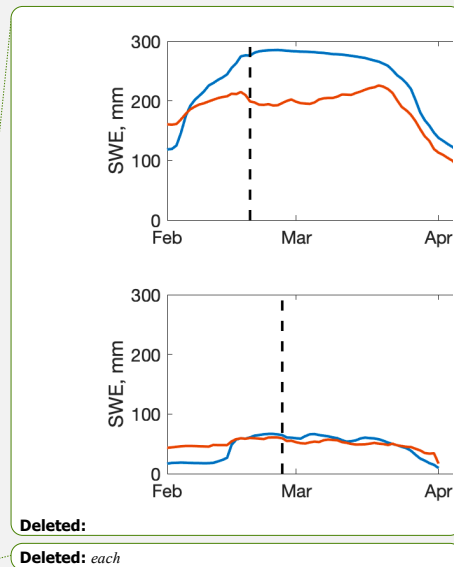


Figure 4 Mean SWE for 2017 (a) and 2018 (b) modeled at all of the AKAH stations using SNOWPACK (blue lines) compared to reconstructed SWE from ParBal using a best of 9-pixel approach (red lines). Also plotted is the median peak SWE date. The hi/lo bounds (filled areas) represent uncertainty. For ParBal, uncertainty is expressed as the range of values in the 9 pixel neighborhood. For SNOWPACK, uncertainty is 5% of the modeled SWE during the ablation season. See Sections 5.1 and 5.2 for details. The modeled SWE values end abruptly on 1 April 2018 because the AKAH stations stopped reporting due to drought conditions. The number of stations used is the same as in Figure 3.



Deleted:

Deleted: each

366  
367

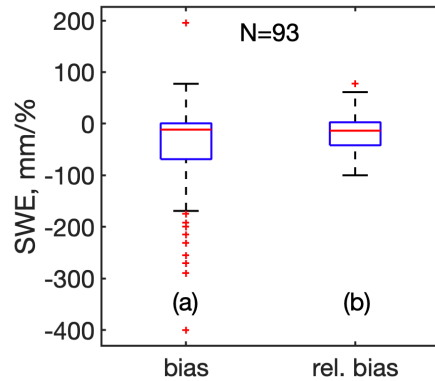


Figure 5 Bias (a) and relative bias (b) error for ParBal reconstructed SWE vs Alpine 3D modeled SWE at AKAH stations the median peak SWE date for both years, where bias here is ParBal SWE – Alpine 3D SWE.

368

369 6.2 Four model spatial comparisons

370 The AKAH stations are lower than the average elevation for the region. The average elevation of  
 371 the AKAH stations is 2619 m (1735 to 3410 m). But when the 500 m DEM is upscaled to 25 km,  
 372 the average elevation of the pixels containing the AKAH station is 3858 m with a range of 2517  
 373 to 4764 m. This has two important implications: 1) much of the higher elevation snowfall is being  
 374 extrapolated and 2) the higher elevation causes the peak SWE date to move forward in time. The  
 375 median peak SWE dates for the (N=169) 25 km pixels encompassing the study area are 5 May  
 376 2017 and 3 May 2017. Thus, we use the median of the two to compare our reconstructed SWE  
 377 values (Figure 6ab, Figure 7a-d, and supplementary video).

Deleted: and

378 Striking is the range between models. NOAH-MP has the highest peaks (562 mm in 2017 and 331  
 379 mm in 2018), but is among the first to melt out. The reconstructed SWE from ParBal only shows  
 380 minor variation between the 2017 peak (240 mm) and the 2018 peak (206 mm). ParBal and  
 381 GLDAS-2 melt snow out latest in both years. This is especially true for ParBal in 2017, where the  
 382 supplementary video shows that ParBal has snow cover over more pixels that persists for longer  
 383 into the melt season, but is lower in SWE than the other models. The Alpine 3D model shows the  
 384 second highest peak SWE in 2017 (469 mm), but the lowest peak (165 mm) in 2018. The  
 385 comparatively higher values from NOAH-MP could result from relatively high precipitation  
 386 estimates from its MERRA2 precipitation forcings. Similarly, Viste and Sorteberg (2015) report  
 387 that MERRA (version 1) showed higher snowfall in the Indus Basin than any other reanalysis or  
 388 observation-based forcings dataset.

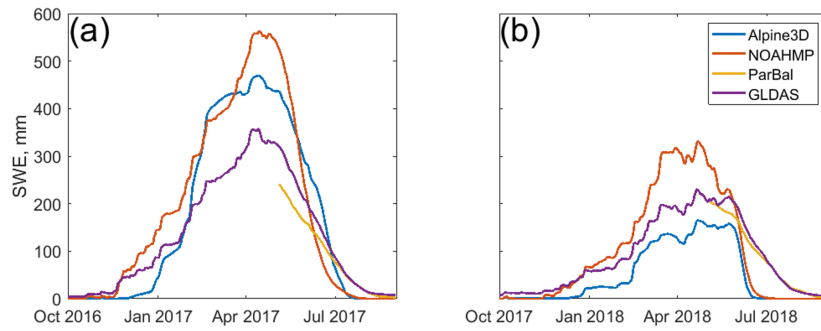


Figure 6 Time series of mean SWE for four snow models across the study area (13x13x25 km pixels) show in Figure 1 for 2017 (a) and 2018 (b). The reconstructed SWE from ParBal (yellow) goes back to 4 May, the median peak SWE date for both years, since reconstruction is only valid during the ablation season.

390



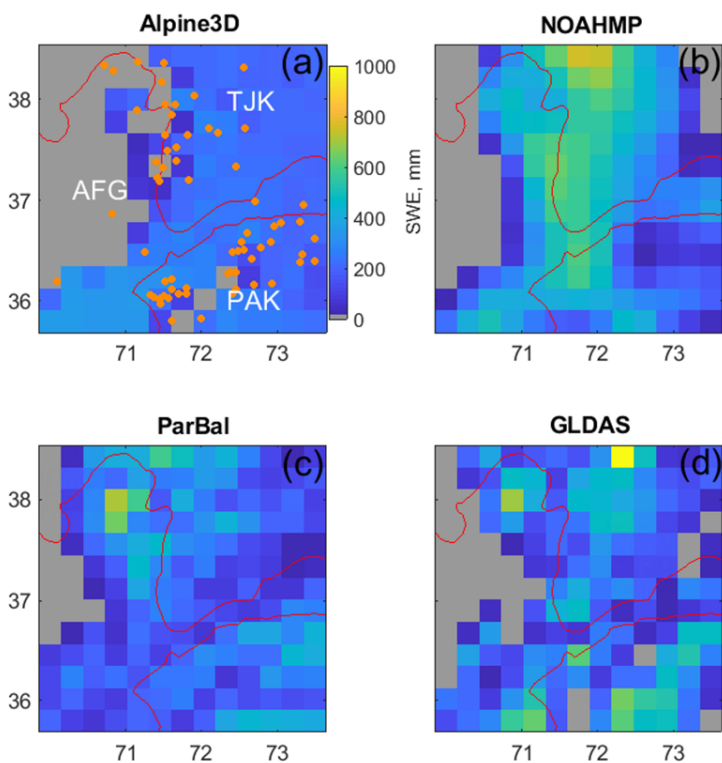


Figure 7 Four model (a-d) spatial comparison for the region on 4 May 2018. The white letters are: AFG–Afghanistan; TJK–Tajikistan; and PAK–Pakistan. Also shown in (a) are the locations of the AKAH stations (orange points). This is a frame from a video sequence available as supplementary material.

Deleted: the 3 letter ISO country codes (

Deleted: )

391 Since Alpine3D is relying heavily on extrapolation of SWE, we suggest its mean SWE values  
 392 plotted in Figure 6 could have higher uncertainty than some of the other models. For example, the  
 393 Alpine3D pixels seem to melt out early compared to the other models, especially ParBal, which is  
 394 the only model relying on satellite-based estimates of fSCA (see supplementary video). Thus,  
 395 Alpine3D may be placing too little SWE in cold, high elevation areas that melt slowly. These  
 396 problems are all indicative of stations that are located in valley bottoms and that only cover the  
 397 lowest elevations across these 25 km pixels.  
 398

399

400 The ParBal results are confounding given that the agreement between the modeled SWE from  
401 ParBal and SNOWPACK at individual AKAH stations (Figure 4ab) is much better for both 2017  
402 and 2018.

403 For insight into potential biases in the modeled spatial SWE from ParBal, we carefully studied the  
404 snow-covered area (SCA, not just for 2017 & 2018, but since 2001), the potential melt (i.e. the  
405 melt if a pixel were 100% snow covered), and the melt from glacierized areas (light blue in Figure  
406 1). We did not find any errors in the model, its parameters, or its forcings. Thus, it is possible that  
407 the ParBal SWE is low-biased in 2017 for reasons that we could not discern, or that the other  
408 models are high biased. Of note is that the 2017 & 2018 SCA (Figure 8 purple and orange) is very  
409 similar for both years during the ablation period, especially at the end of the ablation season.

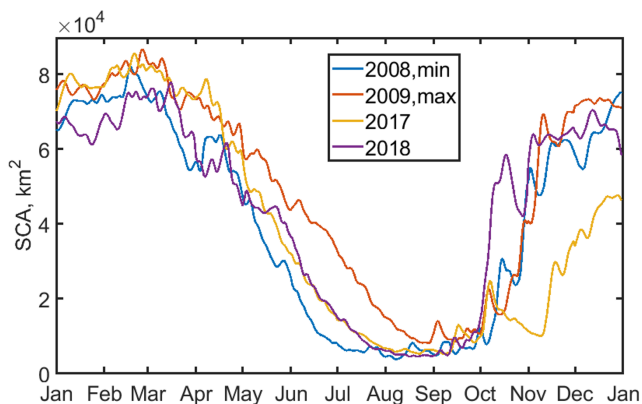


Figure 8 Time series of snow covered area from spatially and temporally interpolated MODSCAG (Rittger et al., in press), an input for ParBal, for four selected years across the region. Years 2008 and 2009 had the lowest and highest values on July 1 over the period of record from 2001 to 2018, while 2017 and 2018 comprise the AKAH station study period.

410 Since pixels do not contribute uniformly to melt, SCA alone cannot be used to predict SWE, but  
411 in general years with less snow have lower SCA values towards the end of the ablation season.  
412 Figure 8 shows that 2017 and 2018 were similar in terms of SCA from April through melt out.  
413 Thus, the large difference between 2017 and 2018 for the AKAH station SWE, but small  
414 differences in SCA and spatially-averaged reconstructed SWE, suggest that 2017 may have been  
415 a larger snow year at the lower elevations where the AKAH stations are, but similar to 2018 at the  
416 higher elevations.  
417

### 418 6.3 Stratigraphy and stability

419 The simulated snow profiles from the AKAH stations (Figure 9ab) and the 25 km pixels containing  
420 the AKAH stations (Figure 10ab) show very different snowpacks. Because of the induced increase  
421 in elevation from scaling (e.g. from an average of 2619 m to 3858 m, Section 6.2), the 25 km pixels  
422 show a deeper, but more faceted snowpack with critical layers that persist for a month or longer.  
423 In 2017, for the median AKAH station values, the snowpack reaches a maximum of 76% facets

424 on January 21 (Figure 9a). In 2018, the snowpack reaches a maximum of 71% facets (Figure 9b).  
 425 There were no critical layers simulated. In contrast, for the median values in the 25 km pixels for  
 426 both years, the height of snow (HS) is approximately  $2 \times$  that for the stations (Figure 10ab). The  
 427 snowpack reaches a maximum of 94% facets in 2017, with one critical layer persisting for 35 days  
 428 (Figure 10a). The snowpack in 2018 reaches 95% facets with 1 or 2 critical layers persisting for  
 429 80 days (Figure 10b). During the Nuristan avalanches on 4 February to 7 February 2017 that killed  
 430 over 100 people (United Nations, 2017), the AKAH stations show the largest 3-day snowfall of  
 431 the study period (Figure 9a) and the results for the 25 km pixels show that large snowfall occurring  
 432 on top of the only critical layer of the season (Figure 9b). That is a classic avalanche scenario, i.e.  
 433 a large snowfall on a weak snowpack.

434 In lieu of any type of snow profile from this region, these profiles paint the best picture of the snow  
 435 conditions available. A relatively stable snowpack seems to be present in the valleys, where the  
 436 AKAH stations are located. But at the higher elevations, the simulated profiles show a more  
 437 dangerous snowpack. This is especially serious considering these villages are in the runout zones  
 438 of these unstable snowpacks. In some cases, several thousand meters of vertical relief loom above  
 439 the villages. For example, Yarkhun Lasht (36.795N 73.022E, el. 3249 m) in Pakistan is flanked by  
 440 6500 m peaks on both side of its valley.

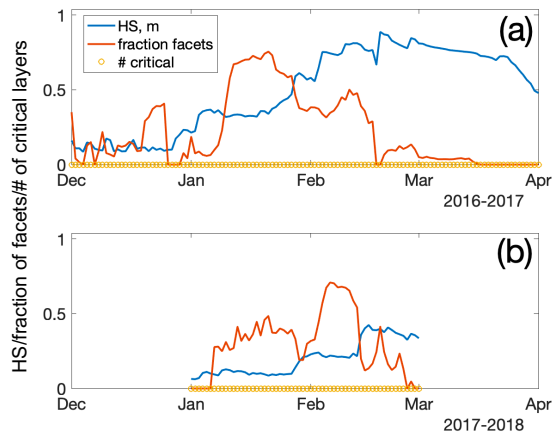


Figure 9 Stratigraphy summary of the AKAH stations for 2017 (a) and 2018 (b). Plotted are the median: height of snow (HS); fraction of the snowpack containing facets; and number of critical layers. The number of stations used to compute the medians varied due to snow coverage.

441

442

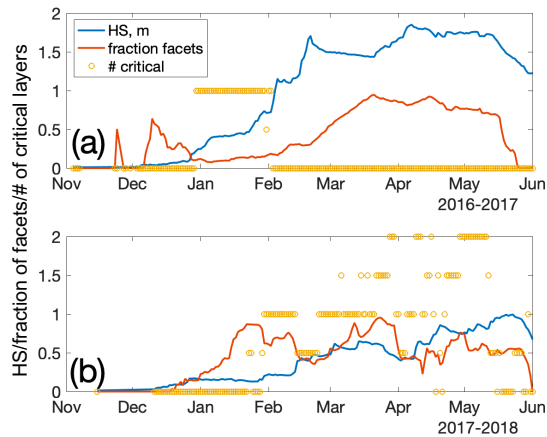


Figure 10 Stratigraphy summary of the (13x13) 25 km pixels containing AKAH stations for 2017 (a) and 2018 (b). Plotted are the median: height of snow (HS); fraction of the snowpack containing facets; and number of critical layers.

443

## 444 7 CONCLUSION

445 Knowledge of the snowpack in northwestern High Mountain Asia is poor. This area is subject to  
446 droughts and threatened by snow avalanches. Both problems can be aided by improved knowledge  
447 of the snowpack. Thanks to a novel operational avalanche observation network, there are now  
448 daily snow measurements at a number of operational weather stations in this austere region. In this  
449 study, two years of daily snow depth measurements from these stations were combined with  
450 downscaled reanalysis and remotely-sensed measurements to force a point and spatially distributed  
451 snow model. Compared to a previous effort (Bair et al., 2018b), this study represents a substantial  
452 improvement in SWE modeling for the region, and a first attempt to characterize region-wide snow  
453 stratigraphy. At the point scale, SWE estimates from a reconstruction technique that does not use  
454 precipitation or in situ measurements compared favorably. At the regional scale, four models  
455 showed a wide spread in both peak SWE and melt timing. For the models that rely on in situ  
456 precipitation measurements, a major challenge is spatial extrapolation, as many of the stations are  
457 located in deep valleys. Adding measurements from the mountains above would facilitate more  
458 realistic lapse rates, but these measurements do not currently exist, although they would be  
459 beneficial both for operational avalanche safety and for scientific studies.

460 In the regional comparison, SWE estimates from ParBal were on the low end, but given the model  
461 spread it is difficult to form a consensus estimate. We plan additional in situ validation at other  
462 sites in High Mountain Asia to continue to assess the performance of ParBal there.

463 The simulated profiles showed very different snowpacks. At the point scale at lower elevations in  
464 the valleys, profiles showed fewer facets and almost no critical layers, while at the regional scale

Deleted: an

Deleted: of High Mountain Asia

467 for higher elevations, the profiles showed heavily faceted snowpacks with critical layers that  
468 persisted throughout the winter and spring.

#### 469 8 CODE AND DATA AVAILABILITY

470 The code for ParBal is accessible at: <https://github.com/edwardbair/ParBal>

471 The code for MeteoIO, SNOWPACK, and Alpine3D are accessible at: <https://models.slf.ch/>

472 The code for NOAH-MP is accessible at: [https://ral.ucar.edu/solutions/products/noah-](https://ral.ucar.edu/solutions/products/noah-multiparameterization-land-surface-model-noah-mp-lsm)  
473 [multiparameterization-land-surface-model-noah-mp-lsm](https://ral.ucar.edu/solutions/products/noah-multiparameterization-land-surface-model-noah-mp-lsm)

474 The GLDAS-2 and MERRA-2 forcings are accessible at: <https://disc.gsfc.nasa.gov/>

475 The reconstructed SWE and melt cubes are accessible at:  
476 <ftp://ftp.snow.ucsb.edu/pub/org/snow/products/reconstruction/h23v05/500m/>

477 Unfortunately, the AKAH measurements are not publicly available due to security concerns.  
478 Requests for the dataset should be made through The Aga Khan Agency for Habitat  
479 (<https://www.akdn.org>).

480 **APPENDIX A Detailed model forcings and parameters**

481 *PARBAL*

482 ParBal was configured and forced as described in Bair et al. (2018b); Bair et al. (2016). The model  
 483 time step was 1 hr. The DEM used was the ASTER GDEM version 2 at 1 arc sec (NASA JPL,  
 484 2011), while the canopy type and fraction were taken from the Global Land Survey at 30 m (USGS,  
 485 2009). The shortwave and longwave forcings were downscaled from the CERES SYN edition 4a  
 486 1°/1 hr product (Rutan et al., 2015), while the air temperature, specific humidity, air pressure, and  
 487 wind speeds were downscaled from the GLDAS NOAH version 2.1 0.25°/3 hr product (Cosgrove  
 488 et al., 2003). Time-space smoothed (Dozier et al., 2008; Rittger et al., in press) fSCA and grain  
 489 size from MODSCAG (Painter et al., 2009) was combined with the visible albedo degradation  
 490 from dust in MODDRFS (Painter et al., 2012) to produce snow hourly snow albedo.

491 *NOAH-MP*

492 NOAH-MP v3.6 was run in retrospective mode within the NASA Land Information System (LIS)  
 493 framework. A state vector ensemble (total 30 replicates) was generated by perturbing the forcings  
 494 to account for the state uncertainty during forward propagation of the model. MERRA-2 (Gelaro  
 495 et al., 2017) forcings were utilized with bilinear spatial and linear temporal interpolation. The  
 496 model was run on an equidistant cylindrical grid with 0.25° spatial resolution and a 15 min model  
 497 timestep. The spin-up time extended from May 2002 to May 2016 while the study period was from  
 498 June 2016 to October 2018. The number of maximum layers in the snowpack was 3. Table A1  
 499 provides details of the NOAH-MP scheme options selected. Further details regarding each scheme  
 500 and relevant references can be found at: [https://ral.ucar.edu/solutions/products/noah-](https://ral.ucar.edu/solutions/products/noah-multiparameterization-land-surface-model-noah-mp-lsm)  
 501 [multiparameterization-land-surface-model-noah-mp-lsm](https://ral.ucar.edu/solutions/products/noah-multiparameterization-land-surface-model-noah-mp-lsm).

Physical process/ parameter	Scheme used
Elevation data	SRTM Native
Landcover data	MODIS Native (IGBPNCEP)
Slope, Albedo and Greenness data	NCEP Native
Bottom temperature (lapse-rate correction)	ISLSCP1
Vegetation	dynamic
Canopy stomatal resistance	Ball-Berry
Runoff and groundwater	SIMGM
Surface layer drag coefficient	M-O (General Monin-Obukhov similarity theory)
Supercooled liquid water and frozen soil permeability	NY06
Radiation transfer	gap=F(3D;cosz)
Snow surface albedo	BATS (Biosphere-Atmosphere Transfer Scheme)

Rainfall and snowfall	Jordan91
Snow and soil temperature time	semi-implicit
Lower boundary of soil temperature	Noah

502 *Table A1 Noah-MP v3.6 physical parametrization scheme options utilized in this study.*

503 *SNOWPACK*

504 SNOWPACK v3.50 was run in research mode at a 15 min timestep with hourly outputs for each  
505 of the AKAH stations. Hourly forcings were computed by combining temporally interpolated snow  
506 depth from the AKAH manual measurements with: air temperature, incoming shortwave, reflected  
507 shortwave, incoming longwave, wind speed, and relative humidity from the downscaled ParBal  
508 outputs, as described in Section 5.2. SNOWPACK was only run for periods when measurements  
509 from the AKAH stations were available, Nov/Dec to April/May, depending on the year.

510 Plots were assumed to be level, so forcings without terrain correction were applied except for  
511 shading when the sun was below the local horizon, e.g. a mountain blocking the sun (Dozier and  
512 Frew, 1990). The wind direction, which is not available in GLDAS-2, was fixed at the mean value  
513 from the daily AKAH instantaneous values. The ground temperature was set as the minimum of  
514 the air temperature or -1.5°C when snow cover was present.

515 Aside from setting required parameters and values for inputs and outputs, changes to default  
516 parameters that affected model output are provided in Table A2:

Parameters	Value	Description
TS_DAYS_BETWEEN	0.014666 days	Output hourly values
PRECIP_RATES	FALSE	Output is provided a summed precipitation over the output timestep (1 hr)
SW_MODE	BOTH	Both incoming and reflected (incoming x albedo) are provided
HEIGHT_OF_METEORO_VALUES	2 m	Height of meteorological measurements
HEIGHT_OF_WIND_VALUE	2 m	Height of wind measurements
ENFORCE_MEASURED_SNOW_HEIGHTS	TRUE	Precipitation is calculated using HS
ATMOSPHERIC_STABILITY	NEUTRAL	Neutral conditions are often present in moderate to high wind speeds for mountain terrain (Lehning et al., 2002a; Mitterer and Schweizer, 2013)
MEAS_INCOMING_LONGWAVE	TRUE	Default is to estimate emissivity of the air and incoming longwave from

		other measured parameters (FALSE). Here we provide longwave forcings (TRUE).
--	--	--

517 *Table A2 Model parameters for SNOWPACK*

518 *ALPINE3D*

519 Alpine3D version 3.10 was run using with the outputs produced by SNOWPACK as forcings for  
520 each of the AKAH stations at 25 km resolution. The DEM and land cover (incorrectly labeled land  
521 use in the Alpine3D documentation) data were upscaled from the ParBal data. Alpine3D was run  
522 at an hourly timestep using hourly forcings, with daily outputs using the “enable-eb” switch. Other  
523 switches were set to off, the defaults. The “enable-eb” switch computes the terrain radiation with  
524 shading and terrain reflections (see Alpine 3D documentation at <https://models.slf.ch> for a  
525 description).

526 To extend the length of the model runs, for each AKAH stations, GLDAS-2 precipitation was  
527 appended to periods prior to the first AKAH observation for the year and after the last, as described  
528 in Section 5.5.

529 The forcings were hourly: incoming shortwave, incoming longwave, air temperature, relative  
530 humidity, wind speed, wind direction, reflected shortwave, accumulated precipitation, and ground  
531 temperature.

532 Critical to Alpine3D are the interpolation methods from MeteoIO to spatially distribute  
533 precipitation and other forcings. We found the modeled SWE to be highly dependent on the spatial  
534 interpolation of precipitation. Our initial approach was to explore local (i.e. with a given radius  
535 from a station) and regional (i.e. all AKAH stations) lapse rates in the measured snow depth and  
536 modeled precipitation from SNOWPACK. We found almost no correlation in many of the  
537 measurements, not surprising given the complexity of the terrain and likely existence of  
538 microclimates with substantial influence on precipitation. Without having a good validation source  
539 for spatial precipitation (as is the case for all of High Mountain Asia), we selected an interpolation  
540 method that yielded relatively smooth results, but showed increases in precipitation with elevation.

541 Ultimately, we decided to use an inverse distance weighting scheme with elevation detrending  
542 (IDW LAPSE) and a multilinear option. For this method, the input data are detrended, then the  
543 residuals are spatially interpolated according to an inverse distance weighting scheme. The  
544 detrending uses a multiple linear regression with northing, easting, and altitude. The linear  
545 regression has an iterative method for removing outliers. Finally, values at each cell are retrended  
546 using the multiple linear regression and added to the interpolated residuals.

547 A summary of the interpolation methods, all of which are defined in the MeteoIO documentation  
548 (Bavay and Egger, 2014), is given in Table A3.

Forcing	Spatial interpolation method	Description and notes
Air temperature	IDW_LAPSE	Inverse distance weighting with elevation detrending.



Accumulated precipitation	IDW_LAPSE with multilinear option set to TRUE	See notes above
Relative Humidity	LISTON_RH	See Liston and Elder (2006)
Precipitation phase	PPHASE	Simple splitting at 274.35K
Wind speed	IDW_LAPSE	See above
Incoming longwave radiation	AVG_LAPSE	Average filling with elevation lapse rate
Wind direction	CST	Constant, fixed at average value from AKAH station instantaneous measurements
Pressure	STD_PRESS	Standard atmospheric pressure with elevation

549 *Table A3 Spatial interpolation methods for Alpine3D*

550 The same parameters as in Table A2 for SNOWPACK were used in Alpine3D with changes shown  
551 in Table A4. Other parameters were defaults.

Parameters	Value	Description
CALCULATION_STEP_LENGTH	60 min	1 hr model timestep
ENFORCE_MEASURED_SNOW_HEIGHTS	FALSE	Use accumulated precipitation estimate from SNOWPACK

552 *Table A4 Model parameter changes for Alpine3D from Table A2*

553 AUTHOR CONTRIBUTION

554 DC provided the AKAH dataset. JA ran the NOAH MP simulations. KR prepared the snow surface  
555 properties dataset. EB processed the data and prepared the manuscript.

556 COMPETING INTERESTS

557 The authors declare that they have no conflicts of interest.

558 ACKNOWLEDGMENTS

559 We are grateful to the Aga Khan Agency for Habitat for supplying the first snow measurements in  
560 Afghanistan's watersheds since the 1980s. This work was supported by NASA Awards  
561 80NSSC18K0427, 80NSSC18K1489, NASA 2015 HiMAT, and NNX17AC15G.

562

563 REFERENCES

564 Adam, J. C., Clark, E. A., Lettenmaier, D. P., and Wood, E. F.: Correction of global precipitation  
565 products for orographic effects, *Journal of Climate*, 19, 15-38, doi 10.1175/JCLI3604.1, 2006.

566 Armstrong, R. L., Rittger, K., Brodzik, M. J., and others: Runoff from glacier ice and seasonal snow in  
567 High Asia: separating melt water sources in river flow, *Regional Environmental Change*, 1-13, doi  
568 <https://doi.org/10.1007/s10113-018-1429-0>, 2018.

569 Bair, E. H., Davis, R. E., and Dozier, J.: Hourly mass and snow energy balance measurements from  
570 Mammoth Mountain, CA USA, 2011–2017, *Earth Syst. Sci. Data*, 10, 549-563, doi 10.5194/essd-10-549-  
571 2018, 2018a.

572 Bair, E. H., Simenhois, R., Birkeland, K., and Dozier, J.: A field study on failure of storm snow slab  
573 avalanches, *Cold Regions Science and Technology*, 79-80, 20-28, doi 10.1016/j.coldregions.2012.02.007,  
574 2012.

575 Bair, E. H., Abreu Calfa, A., Rittger, K., and Dozier, J.: Using machine learning for real-time estimates of  
576 snow water equivalent in the watersheds of Afghanistan, *The Cryosphere*, 12, 1579-1594, doi 10.5194/tc-  
577 12-1579-2018, 2018b.

578 Bair, E. H., Rittger, K., Skiles, S. M., and Dozier, J.: An Examination of Snow Albedo Estimates From  
579 MODIS and Their Impact on Snow Water Equivalent Reconstruction, *Water Resources Research*, 55,  
580 7826-7842, doi 10.1029/2019wr024810, 2019.

581 Bair, E. H., Rittger, K., Davis, R. E., Painter, T. H., and Dozier, J.: Validating reconstruction of snow  
582 water equivalent in California's Sierra Nevada using measurements from the NASA Airborne Snow  
583 Observatory, *Water Resources Research*, 52, 8437-8460, doi 10.1002/2016WR018704, 2016.

584 Bartelt, P., and Lehning, M.: A physical SNOWPACK model for the Swiss avalanche warning: Part I:  
585 numerical model, *Cold Regions Science and Technology*, 35, 123-145, doi 10.1016/s0165-  
586 232x(02)00074-5, 2002.

587 Bavay, M., and Egger, T.: MeteorIO 2.4.2: a preprocessing library for meteorological data, *Geosci. Model*  
588 *Dev.*, 7, 3135-3151, doi 10.5194/gmd-7-3135-2014, 2014.

589 Bellaire, S., Jamieson, J. B., and Fierz, C.: Forcing the snow-cover model SNOWPACK with forecasted  
590 weather data, *The Cryosphere*, 5, 1115-1125, doi 10.5194/tc-5-1115-2011, 2011.

591 Bellaire, S., van Herwijnen, A., Bavay, M., and Schweizer, J.: Distributed modeling of snow cover  
592 instability at regional scale, *Proceedings of the 2018 International Snow Science Workshop, Innsbruck,*  
593 *Austria*, 2018, 871-875,

594 Bookhagen, B., and Burbank, D. W.: Toward a complete Himalayan hydrological budget: Spatiotemporal  
595 distribution of snowmelt and rainfall and their impact on river discharge, *Journal of Geophysical*  
596 *Research: Earth Surface*, 115, doi 10.1029/2009jg001426, 2010.

597 Broxton, P. D., Zeng, X., and Dawson, N.: Why Do Global Reanalyses and Land Data Assimilation  
598 Products Underestimate Snow Water Equivalent?, *J. Hydrometeorol.*, 17, 2743-2761, doi 10.1175/jhm-d-  
599 16-0056.1, 2016.

600 Burt, P., and Adelson, E.: The Laplacian pyramid as a compact image code, *IEEE Transactions on*  
601 *Communications*, 31, 532-540, doi 10.1109/TCOM.1983.1095851, 1983.

602 Chabot, D., and Kaba, A.: Avalanche forecasting in the central Asian countries of Afghanistan, Pakistan  
603 and Tajikistan, Proc. 2016 Intl. Snow Sci. Wksp., Breckenridge, CO, 2016,  
604 <http://arc.lib.montana.edu/snow-science/item/2310>.

605 Chen, F., Barlage, M., Tewari, M., Rasmussen, R., Jin, J., Lettenmaier, D., Livneh, B., Lin, C., Miguez-  
606 Macho, G., Niu, G.-Y., Wen, L., and Yang, Z.-L.: Modeling seasonal snowpack evolution in the complex  
607 terrain and forested Colorado Headwaters region: A model intercomparison study, Journal of Geophysical  
608 Research: Atmospheres, 119, 13,795-713,819, doi 10.1002/2014jd022167, 2014.

609 Cornwell, E., Molotch, N. P., and McPhee, J.: Spatio-temporal variability of snow water equivalent in the  
610 extra-tropical Andes Cordillera from distributed energy balance modeling and remotely sensed snow  
611 cover, Hydrol. Earth Syst. Sci., 20, 411-430, doi 10.5194/hess-20-411-2016, 2016.

612 Cosgrove, B. A., Lohmann, D., Mitchell, K. E., Houser, P. R., Wood, E. F., Schaake, J. C., Robock, A.,  
613 Marshall, C., Sheffield, J., Duan, Q., Luo, L., Higgins, R. W., Pinker, R. T., Tarpley, J. D., and Meng, J.:  
614 Real-time and retrospective forcing in the North American Land Data Assimilation System (NLDAS)  
615 project, Journal of Geophysical Research: Atmospheres, 108, 8842, doi 10.1029/2002JD003118, 2003.

616 Dahri, Z. H., Ludwig, F., Moors, E., Ahmad, B., Khan, A., and Kabat, P.: An appraisal of precipitation  
617 distribution in the high-altitude catchments of the Indus basin, Science of The Total Environment, 548-  
618 549, 289-306, doi <https://doi.org/10.1016/j.scitotenv.2016.01.001>, 2016.

619 Dahri, Z. H., Moors, E., Ludwig, F., Ahmad, S., Khan, A., Ali, I., and Kabat, P.: Adjustment of  
620 measurement errors to reconcile precipitation distribution in the high-altitude Indus basin, Int. J.  
621 Climatol., 38, 3842-3860, doi 10.1002/joc.5539, 2018.

622 Dozier, J., and Frew, J.: Rapid calculation of terrain parameters for radiation modeling from digital  
623 elevation data, IEEE Transactions on Geoscience and Remote Sensing, 28, 963-969, doi  
624 10.1109/36.58986, 1990.

625 Dozier, J., Painter, T. H., Rittger, K., and Frew, J. E.: Time-space continuity of daily maps of fractional  
626 snow cover and albedo from MODIS, Advances in Water Resources, 31, 1515-1526, doi  
627 10.1016/j.advwatres.2008.08.011, 2008.

628 Ek, M. B., Mitchell, K. E., Lin, Y., Rogers, E., Grunmann, P., Koren, V., Gayno, G., and Tarpley, J. D.:  
629 Implementation of Noah land surface model advances in the National Centers for Environmental  
630 Prediction operational mesoscale Eta model, Journal of Geophysical Research: Atmospheres, 108, doi  
631 10.1029/2002jd003296, 2003.

632 Fierz, C., Armstrong, R. L., Durand, Y., Etchevers, P., Greene, E., McClung, D. M., Nishimura, K.,  
633 Satyawali, P. K., and Sokratov, S.: The International Classification for Seasonal Snow on the Ground,  
634 IHP-VII Technical Documents in Hydrology N°83, 90, 2009.

635 Gelaro, R., McCarty, W., Suárez, M. J., Todling, R., Molod, A., Takacs, L., Randles, C. A., Darmenov,  
636 A., Bosilovich, M. G., Reichle, R., Wargan, K., Coy, L., Cullather, R., Draper, C., Akella, S., Buchard,  
637 V., Conaty, A., Silva, A. M. d., Gu, W., Kim, G.-K., Koster, R., Lucchesi, R., Merkova, D., Nielsen, J. E.,  
638 Partyka, G., Pawson, S., Putman, W., Rienecker, M., Schubert, S. D., Sienkiewicz, M., and Zhao, B.: The  
639 Modern-Era Retrospective Analysis for Research and Applications, Version 2 (MERRA-2), Journal of  
640 Climate, 30, 5419-5454, doi 10.1175/jcli-d-16-0758.1, 2017.

- 641 Goodison, B., Louie, P. Y. T., and Yang, D.: WMO Solid precipitation measurement intercomparison,  
642 World Meteorological Organization, 1998.
- 643 Harris, I., Jones, P. D., Osborn, T. J., and Lister, D. H.: Updated high-resolution grids of monthly climatic  
644 observations – the CRU TS3.10 Dataset, *Int. J. Climatol.*, 34, 623-642, doi 10.1002/joc.3711, 2014.
- 645 Hirashima, H., Yamaguchi, S., Sato, A., and Lehning, M.: Numerical modeling of liquid water movement  
646 through layered snow based on new measurements of the water retention curve, *Cold Regions Science  
647 and Technology*, 64, 94-103, doi <https://doi.org/10.1016/j.coldregions.2010.09.003>, 2010.
- 648 Huffman, G. J., Bolvin, D. T., Nelkin, E. J., Wolff, D. B., Adler, R. F., Gu, G., Hong, Y., Bowman, K. P.,  
649 and Stocker, E. F.: The TRMM Multisatellite Precipitation Analysis (TMPA): Quasi-Global, Multiyear,  
650 Combined-Sensor Precipitation Estimates at Fine Scales, *J. Hydrometeorol.*, 8, 38-55, doi  
651 10.1175/jhm560.1, 2007.
- 652 Immerzeel, W. W., Wanders, N., Lutz, A. F., Shea, J. M., and Bierkens, M. F. P.: Reconciling high-  
653 altitude precipitation in the upper Indus basin with glacier mass balances and runoff, *Hydrol. Earth Syst.  
654 Sci.*, 19, 4673-4687, doi 10.5194/hess-19-4673-2015, 2015.
- 655 Jamieson, J. B.: The compression test – after 25 years, *The Avalanche Review*, 18, 10-12, 1999.
- 656 Jepsen, S. M., Molotch, N. P., Williams, M. W., Rittger, K. E., and Sickman, J. O.: Interannual variability  
657 of snowmelt in the Sierra Nevada and Rocky Mountains, United States: Examples from two alpine  
658 watersheds, *Water Resources Research*, 48, W02529, doi 10.1029/2011WR011006, 2012.
- 659 Kochendorfer, J., Rasmussen, R., Wolff, M., Baker, B., Hall, M. E., Meyers, T., Landolt, S., Jachcik, A.,  
660 Isaksen, K., Brækkan, R., and Leeper, R.: The quantification and correction of wind-induced precipitation  
661 measurement errors, *Hydrol. Earth Syst. Sci.*, 21, 1973-1989, doi 10.5194/hess-21-1973-2017, 2017.
- 662 Lehning, M., Bartelt, P., Brown, B., and et. al: SNOWPACK model calculations for avalanche warning  
663 based upon a new network of weather and snow stations, *Cold Reg. Sci. Technol.*, 30, 145-157, 1999.
- 664 Lehning, M., Bartelt, P., Brown, B., and Fierz, C.: A physical SNOWPACK model for the Swiss  
665 avalanche warning: Part III: meteorological forcing, thin layer formation and evaluation, *Cold Regions  
666 Science and Technology*, 35, 169-184, doi 10.1016/S0165-232X(02)00072-1, 2002a.
- 667 Lehning, M., Bartelt, P., Brown, B., Fierz, C., and Satyawali, P.: A physical SNOWPACK model for the  
668 Swiss avalanche warning, Part II: Snow microstructure, *Cold Regions Science and Technology*, 35, 147-  
669 167, doi: 110.1016/S0165-1232X(1002)00073-00073, 2002b.
- 670 Lehning, M., Völsch, I., Gustafsson, D., Nguyen, T. A., Stähli, M., and Zappa, M.: ALPINE3D: a  
671 detailed model of mountain surface processes and its application to snow hydrology, *Hydrological  
672 Processes*, 20, 2111-2128, doi 10.1002/hyp.6204, 2006.
- 673 Liston, G. E., and Elder, K.: A meteorological distribution system for high-resolution terrestrial modeling  
674 (MicroMet), *J. Hydrometeorol.*, 7, 217–234, doi 10.1175/JHM486.1, 2006.
- 675 Lutz, A. F., Immerzeel, W. W., Shrestha, A. B., and Bierkens, M. F. P.: Consistent increase in High  
676 Asia’s runoff due to increasing glacier melt and precipitation, *Nature Climate Change*, 4, 587, doi  
677 10.1038/nclimate2237, 2014.

678 Margulis, S. A., Cortés, G., Giroto, M., and Durand, M.: A Landsat-Era Sierra Nevada Snow Reanalysis  
679 (1985–2015), *J. Hydrometeorol.*, 17, 1203-1221, doi 10.1175/jhm-d-15-0177.1, 2016.

680 Marks, D., and Dozier, J.: Climate and energy exchange at the snow surface in the alpine region of the  
681 Sierra Nevada, 2, *Snow cover energy balance*, *Water Resources Research*, 28, 3043-3054, doi  
682 10.1029/92WR01483, 1992.

683 Martinec, J., and Rango, A.: Areal distribution of snow water equivalent evaluated by snow cover  
684 monitoring, *Water Resources Research*, 17, 1480-1488, doi 10.1029/WR017i005p01480, 1981.

685 Milly, P. C. D., and Dunne, K. A.: Macroscale water fluxes I. Quantifying errors in the estimation of  
686 basin mean precipitation, *Water Resources Research*, 38, 23-21-23-14, doi 10.1029/2001WR000759,  
687 2002.

688 Mitterer, C., and Schweizer, J.: Analysis of the snow-atmosphere energy balance during wet-snow  
689 instabilities and implications for avalanche prediction, *The Cryosphere*, 7, 205-216, doi 10.5194/tc-7-205-  
690 2013, 2013.

691 Molotch, N. P.: Reconstructing snow water equivalent in the Rio Grande headwaters using remotely  
692 sensed snow cover data and a spatially distributed snowmelt model, *Hydrological Processes*, 23, 1076-  
693 1089, doi 10.1002/hyp.7206, 2009.

694 Monti, F., Schweizer, J., and Fierz, C.: Hardness estimation and weak layer detection in simulated snow  
695 stratigraphy, *Cold Regions Science and Technology*, 103, 82-90, doi  
696 <https://doi.org/10.1016/j.coldregions.2014.03.009>, 2014.

697 Nishimura, K., Baba, E., Hirashima, H., and Lehning, M.: Application of the snow cover model  
698 SNOWPACK to snow avalanche warning in Niseko, Japan, *Cold Regions Science and Technology*, 43,  
699 62-70, doi <https://doi.org/10.1016/j.coldregions.2005.05.007>, 2005.

700 Niu, G.-Y., and Yang, Z.-L.: Effects of vegetation canopy processes on snow surface energy and mass  
701 balances, *Journal of Geophysical Research: Atmospheres*, 109, doi 10.1029/2004jd004884, 2004.

702 Niu, G.-Y., Yang, Z.-L., Mitchell, K. E., Chen, F., Ek, M. B., Barlage, M., Kumar, A., Manning, K.,  
703 Niyogi, D., Rosero, E., Tewari, M., and Xia, Y.: The community Noah land surface model with  
704 multiparameterization options (Noah-MP): 1. Model description and evaluation with local-scale  
705 measurements, *Journal of Geophysical Research: Atmospheres*, 116, doi 10.1029/2010jd015139, 2011.

706 Painter, T. H., Bryant, A. C., and Skiles, S. M.: Radiative forcing by light absorbing impurities in snow  
707 from MODIS surface reflectance data, *Geophysical Research Letters*, 39, L17502, doi  
708 10.1029/2012GL052457, 2012.

709 Painter, T. H., Rittger, K., McKenzie, C., Slaughter, P., Davis, R. E., and Dozier, J.: Retrieval of subpixel  
710 snow-covered area, grain size, and albedo from MODIS, *Remote Sensing of Environment*, 113, 868-879,  
711 doi 10.1016/j.rse.2009.01.001, 2009.

712 Painter, T. H., Berisford, D. F., Boardman, J. W., Bormann, K. J., Deems, J. S., Gehrke, F., Hedrick, A.,  
713 Joyce, M., Laidlaw, R., Marks, D., Mattmann, C., McGurk, B., Ramirez, P., Richardson, M., Skiles, S.  
714 M., Seidel, F. C., and Winstral, A.: The Airborne Snow Observatory: Fusion of scanning lidar, imaging  
715 spectrometer, and physically-based modeling for mapping snow water equivalent and snow albedo,  
716 *Remote Sensing of Environment*, 184, 139-152, doi 10.1016/j.rse.2016.06.018, 2016.

717 Raup, B., Racoviteanu, A., Khalsa, S. J. S., Helm, C., Armstrong, R., and Arnaud, Y.: The GLIMS  
718 geospatial glacier database: A new tool for studying glacier change, *Global and Planetary Change*, 56,  
719 101-110, doi <https://doi.org/10.1016/j.gloplacha.2006.07.018>, 2007.

720 Rienecker, M. M., Suarez, M. J., Gelaro, R., Todling, R., Julio Bacmeister, Liu, E., Bosilovich, M. G.,  
721 Schubert, S. D., Takacs, L., Kim, G.-K., Bloom, S., Chen, J., Collins, D., Conaty, A., Silva, A. d., Gu, W.,  
722 Joiner, J., Koster, R. D., Lucchesi, R., Molod, A., Owens, T., Pawson, S., Pegion, P., Redder, C. R.,  
723 Reichle, R., Robertson, F. R., Ruddick, A. G., Sienkiewicz, M., and Woollen, J.: MERRA: NASA's  
724 Modern-Era Retrospective Analysis for Research and Applications, *Journal of Climate*, 24, 3624-3648,  
725 doi 10.1175/jcli-d-11-00015.1, 2011.

726 Rittger, K., Bair, E. H., Kahl, A., and Dozier, J.: Spatial estimates of snow water equivalent from  
727 reconstruction, *Advances in Water Resources*, 94, 345-363, doi 10.1016/j.advwatres.2016.05.015, 2016.

728 Rittger, K., Raleigh, M. S., Dozier, J., Hill, A. F., Lutz, J. A., and Painter, T. H.: Canopy Adjustment and  
729 Improved Cloud Detection for Remotely Sensed Snow Cover Mapping, *Water Resources Research*, in  
730 press.

731 Rodell, M., Houser, P. R., Jambor, U., Gottschalck, J., Mitchell, K., Meng, C. J., Arsenault, K., Cosgrove,  
732 B., Radakovich, J., Bosilovich, M., Entin, J. K., Walker, J. P., Lohmann, D., and Toll, D.: The Global  
733 Land Data Assimilation System, *Bulletin of the American Meteorological Society*, 85, 381-394, doi  
734 10.1175/BAMS-85-3-381, 2004.

735 Rutan, D. A., Kato, S., Doelling, D. R., Rose, F. G., Nguyen, L. T., Caldwell, T. E., and Loeb, N. G.:  
736 CERES synoptic product: Methodology and validation of surface radiant flux, *J. Atmos. Ocean. Technol.*,  
737 32, 1121-1143, doi 10.1175/JTECH-D-14-00165.1, 2015.

738 Schweizer, J., and Jamieson, B.: Snow cover properties for skier triggering of avalanches, *Cold Regions  
739 Science and Technology*, 33, 207-221, doi 10.1016/s0165-232x(01)00039-8, 2001.

740 Schweizer, J., and Jamieson, B.: A threshold sum approach to stability evaluation of manual snow  
741 profiles, *Cold Regions Science and Technology*, 47, 50-59, doi 10.1016/j.coldregions.2006.08.011, 2007.

742 Shakoor, A., and Ejaz, N.: Flow Analysis at the Snow Covered High Altitude Catchment via Distributed  
743 Energy Balance Modeling, *Scientific Reports*, 9, 4783, doi 10.1038/s41598-019-39446-1, 2019.

744 Skiles, S. M., and Painter, T.: Daily evolution in dust and black carbon content, snow grain size, and  
745 snow albedo during snowmelt, *Rocky Mountains, Colorado, Journal of Glaciology*, 63, 118-132, doi  
746 10.1017/jog.2016.125, 2016.

747 Smith, T., and Bookhagen, B.: Changes in seasonal snow water equivalent distribution in High Mountain  
748 Asia (1987 to 2009), *Science Advances*, 4, e1701550, doi 10.1126/sciadv.1701550, 2018.

749 Sturm, M., Holmgren, J., and Liston, G. E.: A seasonal snow cover classification system for local to  
750 global applications, *Journal of Climate*, 8, 1261-1283, doi 10.1175/1520-  
751 0442(1995)008<1261:ASSCCS>2.0.CO;2, 1995.

752 Sturm, M., Taras, B., Liston, G. E., Derksen, C., Jonas, T., and Lea, J.: Estimating snow water equivalent  
753 using snow depth data and climate classes, *J. Hydrometeorol.*, 11, 1380-1394, doi  
754 10.1175/2010jhm1202.1, 2010.

755 Tan, B., Woodcock, C. E., Hu, J., Zhang, P., Ozdogan, M., Huang, D., Yang, W., Knyazikhin, Y., and  
756 Myneni, R. B.: The impact of gridding artifacts on the local spatial properties of MODIS data:  
757 Implications for validation, compositing, and band-to-band registration across resolutions, *Remote*  
758 *Sensing of Environment*, 105, 98-114, doi 10.1016/j.rse.2006.06.008, 2006.

759 United Nations: Afghanistan: Nuristan avalanche, update to flash report (as of 8 February 2017), Office  
760 for the Coordination of Humanitarian Affairs (OCHA), 2017.

761 USAID: Afghanistan Food Security Update, FEWS Net, Washington, DC, 4, 2008.

762 USGS: Global Land Survey: <http://glcfapp.glcf.umd.edu/data/gls/>, access: 1 September 2017, 2009.

763 van Herwijnen, A., and Jamieson, B.: Fracture character in compression tests, *Cold Regions Science and*  
764 *Technology*, 47, 60-68, doi 10.1016/j.coldregions.2006.08.016, 2007.

765 Viste, E., and Sorteberg, A.: Snowfall in the Himalayas: an uncertain future from a little-known past, *The*  
766 *Cryosphere*, 9, 1147-1167, doi 10.5194/tc-9-1147-2015, 2015.

767 Xia, Y., Mitchell, K., Ek, M., Sheffield, J., Cosgrove, B., Wood, E., Luo, L., Alonge, C., Wei, H., Meng,  
768 J., Livneh, B., Lettenmaier, D., Koren, V., Duan, Q., Mo, K., Fan, Y., and Mocko, D.: Continental-scale  
769 water and energy flux analysis and validation for the North American Land Data Assimilation System  
770 project phase 2 (NLDAS-2): 1. Intercomparison and application of model products, *Journal of*  
771 *Geophysical Research: Atmospheres*, 117, D03109, doi 10.1029/2011JD016048, 2012.

772 Xiaoxiong, X., Nianzeng, C., and Barnes, W.: Terra MODIS on-orbit spatial characterization and  
773 performance, *IEEE Transactions on Geoscience and Remote Sensing*, 43, 355-365, doi  
774 10.1109/TGRS.2004.840643, 2005.

775 Yang, Z.-L., and Niu, G.-Y.: The Versatile Integrator of Surface and Atmosphere processes: Part 1.  
776 Model description, *Global and Planetary Change*, 38, 175-189, doi [https://doi.org/10.1016/S0921-](https://doi.org/10.1016/S0921-8181(03)00028-6)  
777 [8181\(03\)00028-6](https://doi.org/10.1016/S0921-8181(03)00028-6), 2003.

778 Yatagai, A., Kamiguchi, K., Arakawa, O., Hamada, A., Yasutomi, N., and Kitoh, A.: APHRODITE:  
779 Constructing a Long-Term Daily Gridded Precipitation Dataset for Asia Based on a Dense Network of  
780 Rain Gauges, *Bulletin of the American Meteorological Society*, 93, 1401-1415, doi 10.1175/bams-d-11-  
781 00122.1, 2012.  
782